



FULL PAPER

Synthesis, crystal structure, and ADME prediction studies of novel imidazopyrimidines as antibacterial and cytotoxic agents

Heba T. Abdel-Mohsen¹ | Amira Abood¹ | Keith J. Flanagan² | Alina Meindl² | Mathias O. Senge² | Hoda I. El Diwani¹

¹Department of Chemistry of Natural and Microbial Products, Division of Pharmaceutical and Drug Industries Research, National Research Centre, Cairo, Egypt

²Medicinal Chemistry, Trinity Translational Medicine Institute, Trinity Centre for Health Sciences, Trinity College Dublin, St. James's Hospital, The University of Dublin, Dublin, Ireland

Correspondence

Heba T. Abdel-Mohsen, Department of Chemistry of Natural and Microbial Products, Division of Pharmaceutical and Drug Industries Research, National Research Centre, El-Buhouth St., Dokki, P.O. Box: 12622, Cairo, Egypt.
Email: hebabdelmohsen@gmail.com and ht.abdel-mohsen@nrc.sci.eg

Funding information

Science Foundation Ireland,
Grant/Award Number: SFI IVP 13/IA/1894

Abstract

In the present study, a novel series of polyfunctionalized imidazopyrimidines **6a–u** and **9a–d** were efficiently constructed by a domino reaction between 2-imino-6-substituted-2,3-dihydropyrimidin-4(1H)-ones **4a–d** or **8a–c** and 2-bromoacetophenones **5a–i** under mild basic conditions. The synthesized series were screened for their antibacterial activity against *Staphylococcus aureus* and *Bacillus subtilis* as Gram-positive (+) bacteria, as well as against Gram-negative (–) bacteria *Escherichia coli*, *Klebsiella pneumoniae*, *Pseudomonas aeruginosa*, and *Salmonella typhi*. Most of the synthesized derivatives of imidazopyrimidines **6** and **9** showed remarkable selectivity against Gram(–) bacteria over the Gram(+) ones. Compounds **6c**, **6f**, and **6g** displayed potent and broad-spectrum antibacterial activity against all tested strains. Compounds **6f** and **6g** displayed promising inhibitory activity on GryB ATPase from *E. coli* with IC₅₀ = 1.14 and 0.73 μM, respectively. Simultaneously, some of the synthesized imidazopyrimidines were screened for their antiproliferative activity against 60 cancer cell lines at a concentration of 10 μM. Compound **9d** showed potent activity against most of the tested cell lines, with a mean growth inhibition of 37%. The ADME (absorption, distribution, metabolism, and excretion) prediction study demonstrated that the synthesized hits have, in addition to their promising chemotherapeutic activity, acceptable pharmacokinetic properties, and a drug-likeness nature to be further developed.

KEYWORDS

ADME, antibacterial activity, antiproliferative activity, imidazopyrimidine

1 | INTRODUCTION

Recently, the emergence of drug-resistant infectious diseases has become one of the most concerning global health problems, resulting in high rates of mortality due to treatment failure.^[1] Overprescription of the currently available antibiotics and low discovery of new antibiotics are the major factors that accelerate the evolution of drug-resistant bacterial infections.^[2] *Staphylococcus aureus*, *Klebsiella pneumoniae*, *Pseudomonas aeruginosa*, followed by *Salmonella* species, are examples of multiresistant bacteria for which new antibiotics are

urgently required.^[3] Therefore, new modes of targeting drug-resistant bacteria are required. One such avenue is targeting the DNA gyrase of bacteria. DNA gyrase, a bacterial type II topoisomerase, is involved in controlling the topological state of DNA in bacteria.^[4] Gyrase enzyme consists of two catalytic subunits in a heterodimer (A₂B₂). GyrA is involved in the breaking and reunion of the double-stranded DNA and GyrB has the adenosine triphosphate (ATP)-binding site and is involved in the hydrolysis of ATP to provide sufficient energy for DNA supercoiling.^[4] Hence, gyrase B is a well-established target for the development of potential novel

antibacterial agents.^[5] Over the last few years, different chemical classes of gyrase B inhibitors that act on ATP-binding sites have been identified.^[6,7] Pyrrolopyrimidines (such as **I**),^[8,9] imidazo[1,2-*a*]pyridines (such as **II**),^[10] benzimidazole ureas (such as **III**),^[11] imidazopyrazinones (such as **IV**),^[12] benzothiazoles (such as **V**),^[13] indazoles (such as **VI**),^[14] 4,5'-bithiazoles (such as **VII**),^[15] and aminopyrimidines (such as **VIII**),^[16] are examples of reported ATP GyrB inhibitors (Figure 1). Despite the achieved progress, many of the identified derivatives fail in clinical trials because of unsatisfactory physicochemical and pharmacokinetic properties.^[17]

Also, resistance to chemotherapeutic agents is regarded as one of the major factors that reduce the efficacy of cancer therapy and lead to the classification of cancer as the second most common cause of death worldwide.^[18] More specifically, pharmacokinetic resistance is responsible for the clinical failure of a high percentage of new and currently existing anticancer agents.^[19]

Considering these facts, there is a challenging requirement to design and synthesize new chemotherapeutic agents with favorable pharmacokinetic profiles to overcome the phenomena of numerous drug resistances. Research is needed in this area to develop newer and safer derivatives of known drugs, as well as to discover newer scaffolds that may have different modes of action.

In this regard, pyrimidines mimic the molecules in the biological systems, and hence, are regarded as important building blocks in the field of drug discovery and development.^[20–25] Recently, Al-Tel and Al-Qawasmeh^[26] reported the synthesis of a novel series of imidazopyrimidines, for example, **IX**, of potent antibacterial activity. Meanwhile, Kamal et al.^[27] demonstrated the promising anticancer activity of some benzimidazole-imidazopyrimidine conjugates such as compound **X** against different cell lines. On the basis of this background and as a continuation of our efforts in the synthesis of new chemotherapeutic agents,^[20,21,23,24,28,29] the main aim of this study is to synthesize a novel series of polyfunctionalized imidazopyrimidines **6** and **9** (Figure 2) that could provide other chemotherapeutic opportunities in drug discovery. The synthesized compounds were evaluated for their antibacterial activity against some Gram-positive (+) and Gram-negative (-) bacteria. The most promising candidates were further evaluated for their inhibitory activity on gyrase B ATPase. Concurrently, some of the synthesized compounds were selected by the National Cancer Institute (NCI) to be screened for their *in vitro* cytotoxic activity. Besides, an *in silico* ADME (absorption, distribution, metabolism, and excretion) prediction study was carried out to predict pharmacokinetic parameters and the drug-likeness nature of the synthesized imidazopyrimidines.

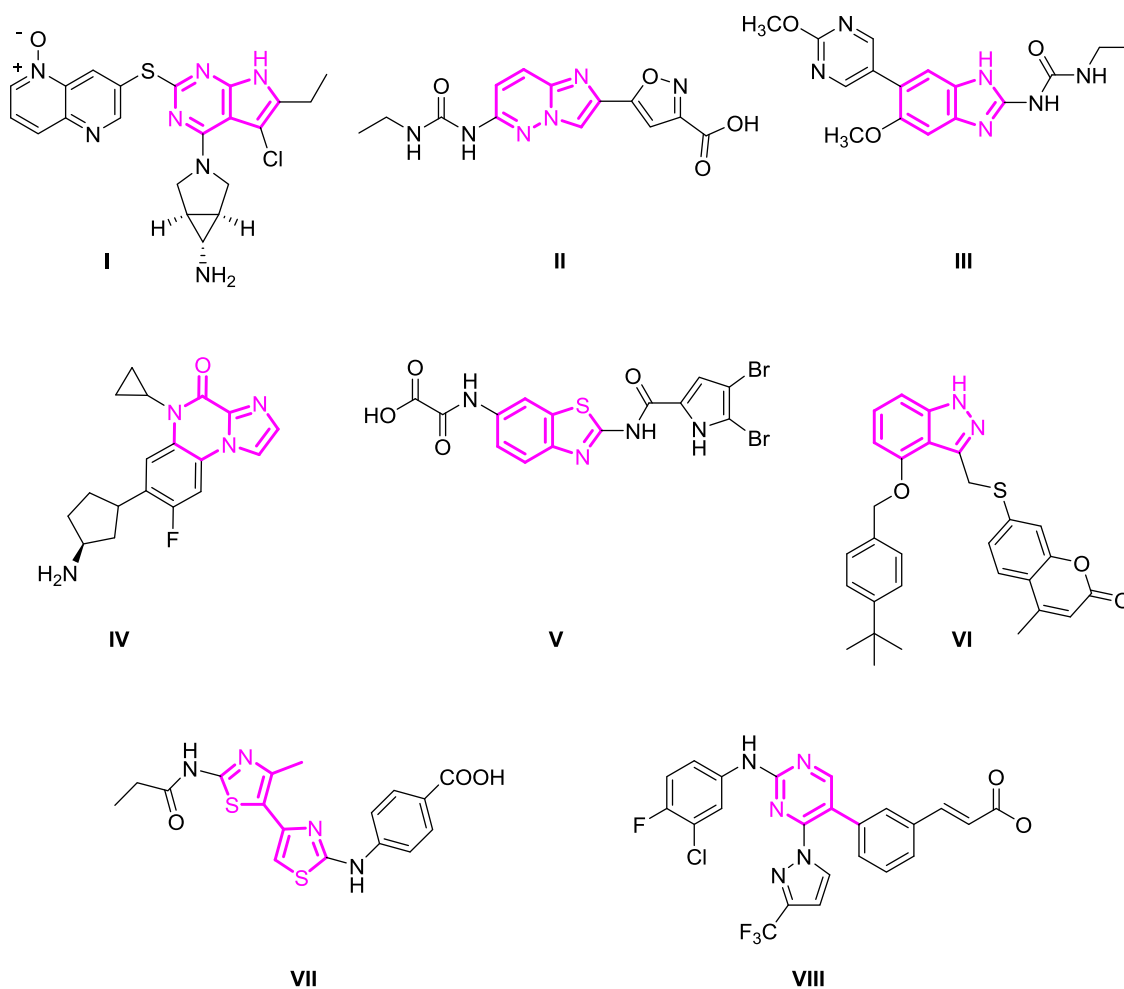


FIGURE 1 Examples of different classes of GyrB inhibitors I-VIII

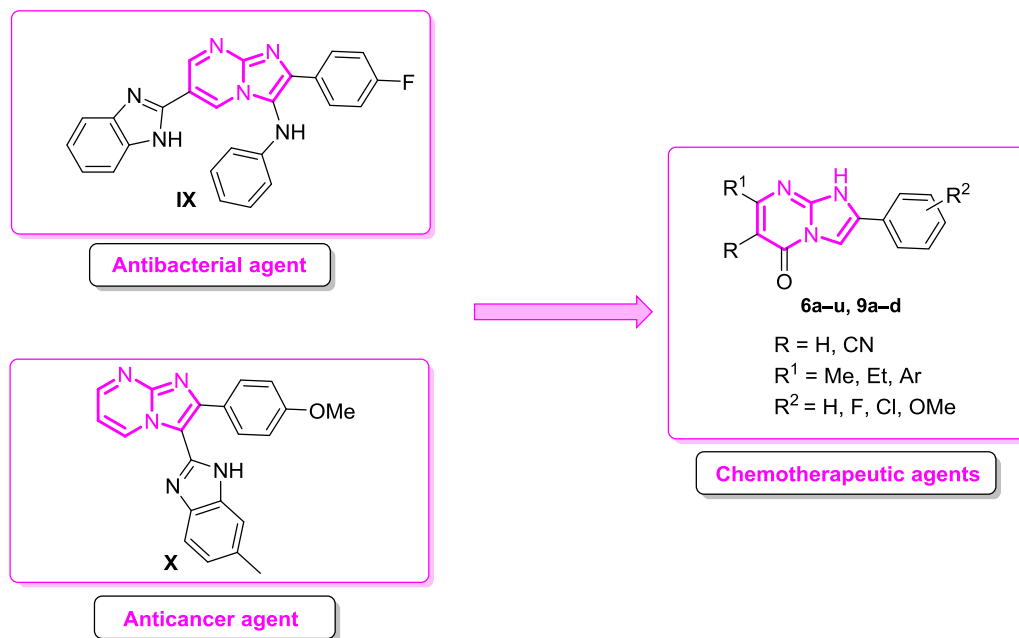


FIGURE 2 Rationale for the design of the new imidazopyrimidines **6a-u** and **9a-d**

2 | RESULTS AND DISCUSSION

2.1 | Chemistry

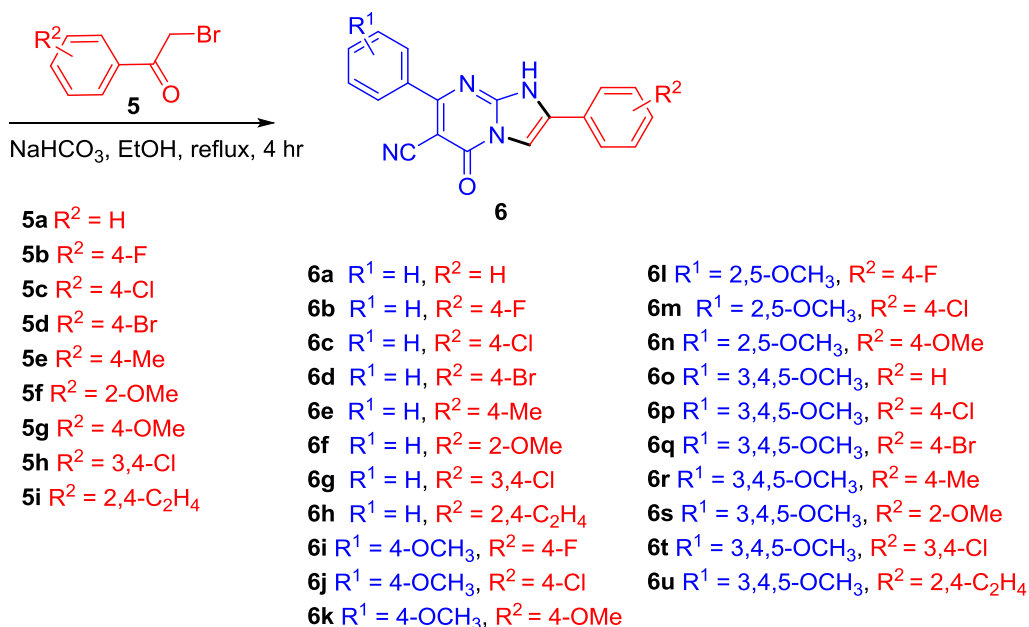
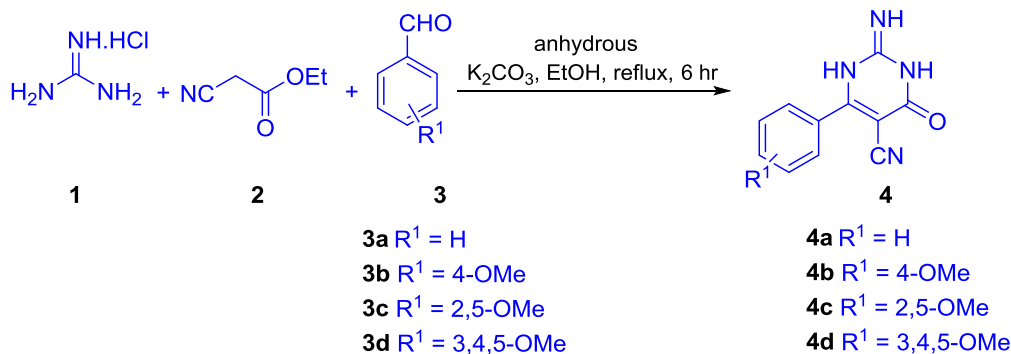
For the synthesis of the target compounds **6a-u**, a series of 2-imino-4-oxo-6-(un)substituted-phenyl-1,2,3,4-tetrahydropyrimidine-5-carbonitriles **4a-d** were first synthesized by one-pot reaction of guanidine hydrochloride (**1**), ethyl cyanoacetate (**2**), and aromatic aldehydes **3a-d** in the presence of anhydrous K_2CO_3 to give the corresponding 2-imino-4-oxo-6-(un)substituted-phenyl-1,2,3,4-tetrahydropyrimidine-5-carbonitriles **4a-d**.^[28] Compounds **4a-d** were subsequently reacted with different 2-bromoacetophenones **5a-i** under basic conditions to give the corresponding cyclized products **6a-u** in good yields under mild reaction conditions (Scheme 1).

On the basis of the higher reactivity of 3-NH over 1-NH^[22,30] it is postulated that the reaction between **4** and **5** proceeds through the initial base-catalyzed nucleophilic substitution reaction of 3-NH of the pyrimidine moiety of **4** with 2-bromoacetophenone **5** to give a tautomeric mixture of the intermediates **A** and **B**. Subsequent intramolecular condensation between the 2-amino group of **B** with C=O afforded the final product **6** exclusively (Scheme 2).

The structures of **6a-u** were elucidated by NMR spectroscopic methods including 2D NMR as well as X-ray crystallographic study. Analysis of the ¹H-NMR spectrum of the reaction between **4** and 2-bromoacetophenones **5** revealed the formation of **6** as an exclusive product. Taking **6p** as an example, ¹H-NMR spectrum showed the presence of three singlets at δ_H 3.76, 3.85, and 7.23 ppm corresponding to 4-OMe, 3,5-OMe, H-2', and H-6' of ring A, respectively; their corresponding directly bonded carbons were identified by gHSQC at δ_C 60.18, 56.00, and 106.24 ppm, respectively. The complete assignment of rings A-D were carried out by gHMBC ¹H-¹³C correlations

optimized for $J_{CH} = 8$ Hz. A strong ³J correlation between three OMe groups at ring A to C-3'', C-4'', and C-5'' allowed the assignment of the latter at δ_C 152.49, 139.56, and 152.49 ppm, respectively. gHMBC showed a strong ³J correlation between H-2'', H-6'', and C-7, which allows its assignment at 165.82 ppm. ¹H-NMR spectrum shows two doublets at δ_H 7.59 and 7.99 ppm corresponding to H-2', H-6' and H-3', H-5', respectively, of ring D. Using gHMBC and gHSQC correlations C-2', C-6' and C-3', C-5' were assigned at δ_C 129.20 and 127.18 ppm, respectively. Strong correlations were seen from H-3' and H-5' to C-1' with H-2', H-6', H-3', and H-5' correlating C-4', which confirms the assignment of C-1' and C-4' at δ_C 130.77 and 134.01 ppm, respectively. A singlet at δ_H 8.49 ppm corresponds to H-3: Its directly bonded carbon was detected by gHSQC at δ_C 105.12 ppm. The quaternary carbons C-2 and C-8a (ring C) were identified by gHMBC correlations; the ³J correlation between H-2', H-6' (δ_H 7.59 ppm) and C-2 established its assignment at δ_C 126.20 ppm whereas a ³J correlations from 3-H to C-8a confirm its assignments at δ_C 146.99 ppm, respectively. The remaining quaternary carbon C-6, C=O, and CN groups were assigned at δ_C 82.64, 156.53, and 117.69 ppm, respectively, by exclusion (Figure 3).

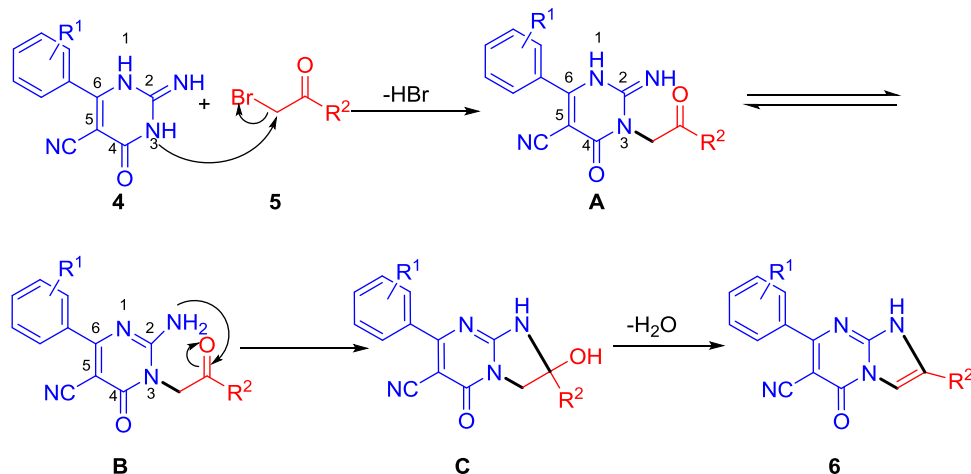
In addition, unequivocal evidence for the structure of **6o** was provided by X-ray crystal structure analysis, and the molecular structure of **6o** is depicted in Figure 4 (for full atom labeling, see Figure S20). In this structure, there are a few features of key interest, namely an intramolecular short hydrogen contact, the solvent (MeOH) hydrogen-bonding network formation, and π -stacking interactions. The intramolecular short hydrogen contact between C14-H14...N4 (2.548[6] Å, 149.6[9]°) results from the almost coplanar orientation of the A and B rings (angle between the planes is 6.2[2]°). As the contact distance is larger than the expected bonding length for a hydrogen bond and the cyano moiety is pointing



SCHEME 1 Synthesis of imidazopyrimidines **6a-u**

away from the CH group, it is clear that this interaction is coincidental with the planar orientation and not its driving force. When looking down the *ac*-plane, a linear arrangement of individual molecular units is formed. A linear hydrogen-bonding network

centered on the imidazopyrimidine ring from the cyano group of one molecule to the amine of its nearest neighbor can be observed. This is facilitated by the incorporation of MeOH solvent molecule between the imidazopyrimidine rings with the amine moiety bonding



SCHEME 2 Proposed mechanism for the synthesis of **6**

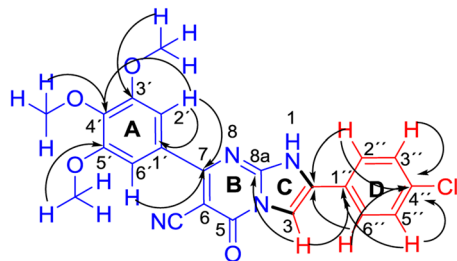


FIGURE 3 Important gHMBC correlations in **6p**

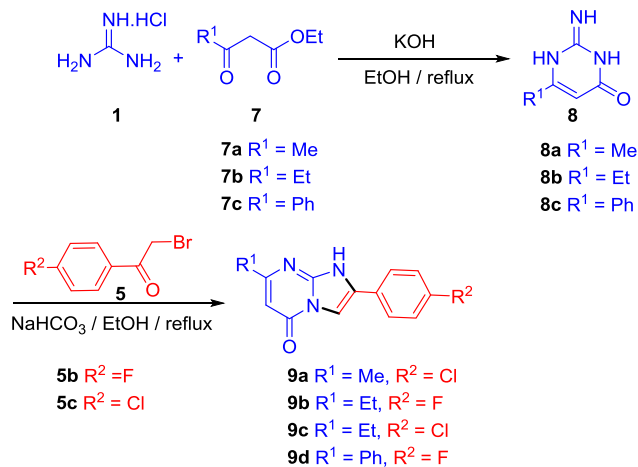
to the oxygen of the MeOH and the cyano motif interacting with the OH hydrogen atom (N2-H2...O1S [1.841{5} Å, 170.8{3}°] and O1S-H1S...N4 [1.960{4} Å, 176.1{7}°]; Figure S21). In the crystal packing, one of the major features observed is the extensive π -stacked system (Figure S22). This is due to the individual layers of the crystal lattice being rotated at $\sim 180^\circ$ to each other, with the tri-methoxybenzene and imidazopyrimidine rings alternately stacking with each other when viewed down the b -axis. As a result of this high planarity within these compounds, it is clear that the formation of such π -stacked networks is a favorable interaction.

After the successful synthesis of **6a-u**, the synthesis of **9a-d** was achieved by initial construction of crucial starting material **8a-c** through a base-catalyzed condensation between guanidine hydrochloride (**1**) and B -ketoesters **7a-c** in the presence of KOH.^[21] Subsequently, **8a-c** were reacted with different 2-bromoacetophenones **5b,c** to give the compounds **9a-d** as single products (Scheme 3).

2.2 | Biological evaluation

2.2.1 | In vitro antimicrobial activity

In the present study, in vitro evaluation of the antimicrobial activities of all the synthesized imidazopyrimidines **6a-u** and **9a-d** against two Gram(+) bacteria (*S. aureus* [ATCC 6538] and *B. subtilis* [ATCC 663]) and four Gram(-) bacteria (*E. coli* [ATCC



SCHEME 3 Synthesis of the target imidazo[1,2- a]pyrimidines **9a-d**

8739], *P. aeruginosa* [ATCC 9027], *S. typhi* [ATCC 14028], and *K. pneumonia* [ATCC 10131]) were performed employing the agar well-diffusion technique.^[31,32] Ampicillin and levofloxacin were used as reference drugs for Gram(+) and Gram(-) bacteria, respectively. The diameters of the inhibition zones (mm) subsequent to treatment with 100 μ l of 10 mg/ml of **6a-u** and **9a-d**, as well as the positive controls are presented in Table 1.

From the results depicted in Table 1, most of the synthesized imidazopyrimidines **6a-u** and **9a-d** showed promising zones of inhibition against Gram(-) bacteria over Gram(+) ones. Concerning the Gram(+) bacteria, *B. subtilis* is much more sensitive to the effect of synthesized compounds rather than *S. aureus*. Most of the compounds having unsubstituted phenyl group **6a-d**, **6f**, **6g** at position-7 showed moderate to potent antimicrobial activity against *S. aureus*, whereas complete loss of activity was observed upon introducing methoxyphenyl groups in **6i**, **6k-u**. Compounds **6e**, **6h**, and **6j** are the only exceptions. Meanwhile, compounds **6i-k** with a 4-methoxyphenyl group at position-7 were more potent than **6a-g** against *B. subtilis*. Compounds **6b-d**, **6f**, **6g**, **6j**, and **9b** showed wider zones of inhibition than ampicillin against *S. aureus*, whereas **6a-g**, **6i-k**, and **9d** demonstrated larger inhibition zones than ampicillin

FIGURE 4 Molecular structure of 5-oxo-2-phenyl-7-(3,4,5-trimethoxyphenyl)-1,5-dihydroimidazo[1,2- a]pyrimidine-6-carbonitrile (**6o**) (thermal displacement 50%)

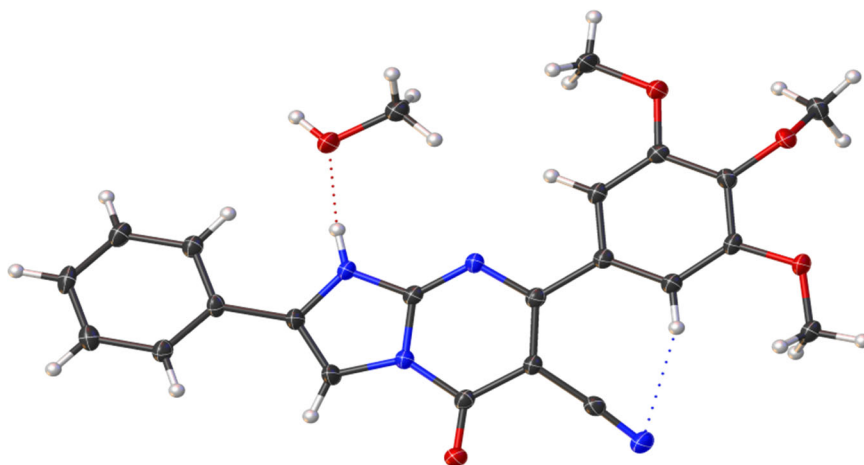


TABLE 1 Antimicrobial activities of **6a–u**, **9a–d**, and positive controls expressed as diameters of inhibition zone (mm)

Entry	Product	Diameter of inhibition zone (mm)					
		Gram(+)		Gram(-)			
		<i>Staphylococcus aureus</i>	<i>Bacillus subtilis</i>	<i>Escherichia coli</i>	<i>Pseudomonas aeruginosa</i>	<i>Klebsiella pneumoniae</i>	<i>Salmonella typhi</i>
1	6a	11±0.0	14±0.7	11.5±0.7	35±1.4	19±5.7	14±0.0
2	6b	15±0.7	21±0.7	16±2.8	-	15±0.7	-
3	6c	16.5±0.7	19±0.0	20.5±0.7	40±0.7	34.5±3.5	23.5±0.7
4	6d	13±0.0	20±1.4	11±0.0	-	16.5±0.7	18.5±0.7
5	6e	-	18±1.4	12±0.0	12±0.0	16±2.8	15±0.0
6	6f	13±0.0	17±2.1	20.5±0.7	16±0.7	14.5±0.7	16.5±0.7
7	6g	13.5±0.7	16±0.7	17.5±0.7	12±0.7	17.5±2.1	15.5±2.1
8	6h	-	-	11±0.0	15±0.7	16.5±0.7	18±2.8
9	6i	-	32±0.7	-	15±1.4	12±0	-
10	6j	17±2.1	25±1.4	20±0	-	20±0.7	14±0.7
11	6k	-	45±0.7	-	-	-	-
12	6l	-	-	-	-	-	14±1.4
13	6m	-	-	-	-	12±0	20±2.8
14	6n	-	-	-	-	-	-
15	6o	-	11±0.7	-	-	16±0.0	19.5±0.7
16	6p	-	-	-	-	17±0.0	16±1.4
17	6q	-	-	13±0.0	11±2.1	15.5±0.7	18±1.4
18	6r	-	12±0.0	11.5±0.7	-	19±0.0	16.5±0.7
19	6s	-	-	11±0.0	-	18±0.0	14.5±0.7
20	6t	-	-	-	-	20±0.0	14.5±0.7
21	6u	-	-	-	-	16±0.0	15±1.4
22	9a	-	-	-	-	15.5±0.7	14±0.0
23	9b	20±0.7	-	25±1.4	17±0	11±1.4	15±0.7
24	9c	-	-	-	-	15.5±0.7	16±1.4
25	9d	-	19±2.1	-	15±2.1	14±0	20±1.4
26	Ampicillin	12±0.7	13±0.0	nd	nd	nd	nd
27	Levofloxacin	nd	nd	20±0.0	14±1.4	20±2.0	11±0.0
28	Dimethyl sulfoxide	-	-	-	-	-	-

against *B. subtilis*. Regarding Gram(-) bacteria, most of the tested compounds possess significant antibacterial activity against *K. pneumoniae* and *S. typhi* in comparison to their effect on *E. coli* and *P. aeruginosa*. Again, most of the compounds exhibiting unsubstituted phenyl group at position-7 **6a–h** showed moderate to potent antimicrobial activity against *E. coli* and *P. aeruginosa*, whereas decrease or complete loss of activity was observed upon introducing methoxyphenyl groups. Compounds **6j** and **6q** are exceptions. Compounds **6c**, **6f**, **6j**, and **9b** were equipotent or more potent than levofloxacin against *E. coli*, whereas **6a**, **6c**, **6f**, **6h**, **6i**, **9b**, and **9d** showed wider zones of inhibition than levofloxacin against *P. aeruginosa*. Nearly all of the tested imidazopyrimidines demonstrated promising activity against *K. pneumoniae* and *S. typhi* in comparison to levofloxacin. Compound **6c** showed the widest zone of inhibition against the two bacterial strains.

On the basis of the obtained results, the minimum inhibitory concentration (MIC) of the synthesized imidazopyrimidines that showed antimicrobial activity was determined by employing a twofold serial dilution technique.^[31,32] The lowest concentration that showed no growth inhibition was determined as the MIC, and the obtained results are presented in Table 2.

Analysis of the obtained results revealed that some imidazopyrimidines have significant inhibitory effects against Gram(+) and Gram(-) bacteria with MIC up to 10 µg/ml. The effect of the substituents at position-2 demonstrated that compound **6c** with *p*-chlorophenyl group exhibited promising antimicrobial activity against all the tested bacteria.

None of the tested imidazopyrimidines showed higher activity than ampicillin against *S. aureus*. From the obtained results, it is obvious that introduction of the 4-F phenyl group in **6b**

TABLE 2 Minimum inhibitory concentrations ($\mu\text{g/ml}$) of synthesized imidazopyrimidines compared to ampicillin and levofloxacin as positive controls

Entry	Product	Minimum inhibitory concentration ($\mu\text{g/ml}$)					
		Gram(+)		Gram(-)			
		<i>Staphylococcus aureus</i>	<i>Bacillus subtilis</i>	<i>Escherichia coli</i>	<i>Pseudomonas aeruginosa</i>	<i>Klebsiella pneumoniae</i>	<i>Salmonella typhi</i>
1	6a	500	500	500	50	50	100
2	6b	500	500	500	-	1,000	-
3	6c	50	50	10	50	12.5	12.5
4	6d	2,500	50	50	-	2,500	50
5	6e	-	500	500	100	100	50
6	6f	50	50	12.5	12.5	50	25
7	6g	500	10	10	50	50	12.5
8	6h	-	-	500	500	500	500
9	6i	-	100	-	500	500	-
10	6j	500	50	50	-	1,000	500
11	6k	-	500	-	-	-	-
12	6l	-	-	-	-	-	25
13	6m	-	-	-	-	2,500	500
14	6n	-	-	-	-	-	-
15	6o	-	500	-	-	500	100
16	6p	-	-	-	-	50	25
17	6q	-	-	1,000	1,000	1,000	100
18	6r	-	500	500	-	500	100
19	6s	-	-	500	-	500	100
20	6t	-	-	-	-	50	12.5
21	6u	-	-	-	-	500	100
22	9a	-	-	-	-	2,500	1,000
23	9b	100	-	50	500	500	1,000
24	9c	-	-	-	-	50	100
25	9d	-	50	-	50	25	12.5
26	Ampicillin	6.25	12.5	nd	nd	nd	nd
27	Levofloxacin	nd	nd	6.25	12.5	10	3.13
28	Dimethyl sulfoxide	-	-	-	-	-	-

(MIC = 500 $\mu\text{g/ml}$) or 3,4-dichlorophenyl group in **6g** (MIC = 500 $\mu\text{g/ml}$) resulted in no change in the antibacterial activity when compared to **6a** (MIC = 500 $\mu\text{g/ml}$), whereas introduction of the 4-Cl phenyl moiety in **6c** (MIC = 50 $\mu\text{g/ml}$) or 2-methoxyphenyl group in **6f** (MIC = 50 $\mu\text{g/ml}$) resulted in 10-fold increase in the potency. Replacement of the 4-chlorophenyl group of **6c** (MIC = 50 $\mu\text{g/ml}$) with 4-bromo derivative in **6d** (MIC = 2,500 $\mu\text{g/ml}$) resulted in a 50-fold decrease in the potency, whereas replacement with 4-tolyl moiety in **6e** or naphthyl moiety in **6h** showed total loss of the antibacterial activity against *S. aureus*.

The MIC results of the synthesized imidazopyrimidines on *B. subtilis* demonstrated that **6g** (MIC = 10 $\mu\text{g/ml}$) has a higher potency than ampicillin (MIC = 12.5 $\mu\text{g/ml}$). Introduction of the 4-F phenyl group in **6b** (MIC = 500 $\mu\text{g/ml}$), 4-tolyl group in **6e** (MIC = 500 $\mu\text{g/ml}$)

resulted in no change in the potency when compared to the 2-phenyl derivative **6a** (MIC = 500 $\mu\text{g/ml}$). Whereas compounds **6c**, **6d**, and **6f**, which exhibit 4-chlorophenyl, 4-bromophenyl, and 2-methoxyphenyl groups, respectively, showed a 10-fold increase in the activity (MIC = 50 $\mu\text{g/ml}$). Further, introduction of the 3,4-dichlorophenyl group in **6g** (MIC = 10 $\mu\text{g/ml}$) demonstrated a fivefold increase in the potency in comparison to **6c** (MIC = 50 $\mu\text{g/ml}$). Replacement of the phenyl moiety in **6a** with naphthyl moiety in **6h** resulted in complete loss of activity. In series **6i-k**, compound **6j** with the *p*-chlorophenyl group at position-2 showed MIC = 50 $\mu\text{g/ml}$. Replacement of the 4-chlorophenyl group in **6j** (MIC = 50 $\mu\text{g/ml}$) with 4-fluorophenyl in **6i** (MIC = 100 $\mu\text{g/ml}$) or 4-methoxyphenyl group in **6k** (MIC = 500 $\mu\text{g/ml}$) resulted in twofold and tenfold decrease in the potency, respectively.

Compounds **6c** (MIC = 10 µg/ml), **6g** (MIC = 10 µg/ml) with chlorophenyl groups, and **6f** (MIC = 12.5 µg/ml) with a 2-methoxyphenyl moiety at position-2 are slightly less potent than levofloxacin (MIC = 6.25 µg/ml) against *E. coli*, whereas **6d**, **6j**, and **9b** showed moderate antibacterial activity (MIC = 50 µg/ml). Replacement of the phenyl group at position-2 of **6a** (MIC = 500 µg/ml) with the 4-F phenyl group in **6b**, 4-tolyl group in **6e** or naphthyl group in **6h** resulted in no change in the activity (MIC = 500 µg/ml), whereas a 10-fold increase in the potency was observed by introduction of 4-Br phenyl group in **6d** (MIC = 50 µg/ml). Further increase in the potency appeared in **6f** (MIC = 12.5 µg/ml), which exhibits the 2-methoxyphenyl group at position-2 and it reaches its maximum potency by the incorporation of the *p*-chlorophenyl group in **6c** (MIC = 10 µg/ml) and the 3,4-dichlorophenyl group in **6g** (MIC = 10 µg/ml).

Compound **6f** (MIC = 12.5 µg/ml) demonstrated comparable antibacterial activity to levofloxacin (MIC = 12.5 µg/ml) against *P. aeruginosa*. Compound **6a** displayed moderate inhibitory activity of MIC = 50 µg/ml, replacement of the phenyl group at position-2 with 4-chlorophenyl group in **6c** or 3,4-dichlorophenyl in **6g** resulted in no change in the activity (MIC = 50 µg/ml), whereas its replacement with 4-tolyl moiety in **6e** (MIC = 100 µg/ml) or naphthyl group in **6h** (MIC = 500 µg/ml) resulted in twofold and tenfold decrease in the potency, respectively. Total loss of potency was observed by introduction of the 4-fluorophenyl group in **6b** or 4-bromophenyl group in **6d**.

K. pneumoniae is one of the most sensitive bacterial strains to the synthesized imidazopyrimidines. Compounds **6c** and **9d** (MIC = 12.5 and 25 µg/ml, respectively) showed potent antibacterial activity against *K. pneumoniae*, whereas compounds **6a**, **6f**, **6g**, **6p**, **6t**, and **9c** showed moderate antibacterial activity (MIC = 50 µg/ml) in comparison to levofloxacin (MIC = 10 µg/ml). In series **6a-h**, replacement of the phenyl group in **6a** (MIC = 50 µg/ml) with the 2-methoxyphenyl group in **6f** or the 3,4-dichlorophenyl group in **6g** (MIC = 50 µg/ml) resulted in no change in the activity, whereas replacement of the phenyl group in **6a** (MIC = 50 µg/ml) with *p*-chlorophenyl group in **6c** displayed increase in the antibacterial activity (MIC = 12.5 µg/ml). On the contrary, introduction of 4-fluorophenyl moiety in **6b** (MIC = 1,000 µg/ml), 4-bromophenyl group in **6d** (MIC = 2,500 µg/ml), 4-tolyl group in **6e** (MIC = 100 µg/ml), or naphthyl group in **6h** (MIC = 500 µg/ml) resulted in decrease in the potency against *K. pneumoniae*. In series **6o-u**, replacement of the phenyl group at position-2 of **6o** (MIC = 500 µg/ml) with a 4-tolyl moiety in **6r**, 2-methoxyphenyl in **6s**, or naphthyl group in **6u** resulted in no change in the potency (MIC = 500 µg/ml), whereas 10-fold increase in the activity appeared upon introduction of the 4-chlorophenyl group in **6p** (MIC = 50 µg/ml) and 3,4-dichlorophenyl group in **6t** (MIC = 50 µg/ml). The 4-bromophenyl derivative **6q** (MIC = 1,000 µg/ml) has a twofold decrease in potency in comparison to **6o** (MIC = 500 µg/ml). In series **9a-d**, compound **9d** (MIC = 25 µg/ml) was the most potent compound in series **9**, replacement of the phenyl group at position-7 of **9d** with ethyl group in **9b** (MIC = 500 µg/ml) resulted in 20-fold decrease in the potency, whereas further replacement of the 4-fluorophenyl group at position-2 of **9b** with 4-chlorophenyl group in **9c** (MIC = 50 µg/ml) resulted in 10-fold increase in the potency. Further replacement of the ethyl group at

position-7 of **9b** (MIC = 500 µg/ml) with a methyl group in **9a** (MIC = 2,500 µg/ml) resulted in a fivefold decrease in the antibacterial activity.

S. typhi is also one of the most sensitive microorganisms to the synthesized series. The imidazopyrimidines **6c**, **6g**, **6t**, and **9d** (MIC = 12.5 µg/ml) were the most potent derivatives. Replacement of the 2-phenyl group of **6a** (MIC = 100 µg/ml) with 4-bromophenyl moiety in **6d** (MIC = 50 µg/ml), 4-tolyl in **6e** (MIC = 50 µg/ml) resulted in a twofold increase in the activity, whereas the incorporation of 2-methoxyphenyl substituent in **6f** (MIC = 25 µg/ml) resulted in a fourfold increase in the potency in comparison to **6a** (MIC = 100 µg/ml), whereas introduction of 4-chlorophenyl substituent in **6c** (MIC = 12.5 µg/ml) or 3,4-dichlorophenyl substituent in **6g** (MIC = 12.5 µg/ml) showed an eightfold increase in the potency. Replacement of the phenyl group of **6a** with a naphthyl moiety in **6h** (MIC = 500 µg/ml) displayed a fivefold decrease in the potency, whereas introduction of the 4-fluorophenyl substituent in **6b** resulted in total loss of the activity. In series **6o-u**, compound **6o** (MIC = 100 µg/ml) with 3,4,5-trimethoxyphenyl group at the position-7 has the same potency as **6a** (MIC = 100 µg/ml) with a phenyl group at position-7. Replacement of the phenyl group at position-7 of **6o** (MIC = 100 µg/ml) with 4-bromophenyl **6q**, 4-tolyl in **6r**, 2-methoxyphenyl in **6s**, or naphthyl in **6u** resulted in no change of the potency, whereas replacement of phenyl group of **6o** (MIC = 100 µg/ml) with 4-chlorophenyl in **6p** (MIC = 25 µg/ml) or 3,4-dichlorophenyl in **6t** (MIC = 12.5 µg/ml) resulted in a fourfold and eightfold increase in the potency, respectively. In series **9**, compounds **9a** and **9b** (MIC = 1,000 µg/ml) showed weak activity, whereas a 10-fold increase in potency was observed by replacement of the 4-fluorophenyl group of **9b** (MIC = 1,000 µg/ml) with 4-chlorophenyl moiety in **9c** (MIC = 100 µg/ml). Further replacement of the aliphatic group at position-7 of **9a-c** (MIC = 100–1,000 µg/ml) with a phenyl group in **9d** showed more than the eightfold increase in potency (MIC = 12.5 µg/ml).

2.2.2 | In vitro inhibitory activity on *E. coli* GyrB ATPase

The most potent compounds **6c**, **6d**, **6f**, **6g**, and **9d**, as well as novobiocin, were evaluated for their GyrB ATPase inhibitory activity using *E. coli* gyrase for ATPase assays kit according to the manufacturers' protocol (Inspiralis Ltd, England) and the results are presented in Table 3. From the obtained results, it is obvious that the

TABLE 3 Inhibitory activity of imidazopyrimidines on *Escherichia coli* gyrase B ATPase

Entry	Compound	IC ₅₀ (µM) ^a on GyrB ATPase
1	6c	1.52
2	6d	>10
3	6f	1.14
4	6g	0.73
5	9d	>10
6	Novobiocin	0.05

^aResults are average of two independent experiments.

imidazopyrimidine derivatives **6c**, **6f**, and **6g** bearing 4-chlorophenyl, dichlorophenyl, or 2-methoxyphenyl substituents at position-2 showed GyrB ATPase inhibitory activity of $IC_{50} = 1.52$, 1.14 , and $0.73 \mu\text{M}$, respectively in comparison to novobiocin ($IC_{50} = 0.05 \mu\text{M}$), whereas compounds **6d** and **9d** showed $IC_{50} > 10 \mu\text{M}$.

2.2.3 | In vitro antiproliferative activity against NCI 60-cell line panel

Some of the synthesized imidazopyrimidines were screened for their in vitro antiproliferative activity through the Developmental Therapeutics Program of NCI in the division of cancer treatment and diagnosis (NIH, Bethesda, MD; www.dtp.nci.nih.gov). This involved screening the synthesized compounds at a single dose of $10 \mu\text{M}$ against a full-NCI 60-cell panel including leukemia, melanoma, lung, colon, brain, ovary, kidney, prostate, and breast cancers. The results are presented in Table 4.

From the obtained results, it was clear that each of the synthesized imidazopyrimidine has a different degree of efficiency against 60 cancer cell lines. NCI-H522 from non-small-cell lung cancer, SNB-75 from central nervous system (CNS) cancer, UO-31 from renal cancer, and MCF-7 and T-47D from breast cancer are the most sensitive cell lines to the tested imidazopyrimidines **6a-d**, **6f-h**, **6p**, and **9d**. Compound **9d** showed a broad spectrum of promising antiproliferative activity against several NCI cell panels with a mean growth inhibition percentage of 37%. At $10 \mu\text{M}$ concentration, **9d** exerted 44%, 81%, 81%, 60%, and 84% growth inhibition against the leukemia cell lines CCRF-CEM, HL-60, K-562, MOLT-4, and SR, respectively; 45%, 53%, and 64% of inhibition against non-small-cell lung cancer cell lines HOP-92, NCI-H460, and NCI-H522, respectively; 49%, 62%, 59%, 56%, and 60% of inhibition against HCT-116, HCT-15, HT29, KM12, and SW-620, respectively, from colon cancer; 54% and 44% against SF-295 and U251 from CNS cancer; 50%, lethal effect, 45%, and 63% of inhibition against M14, MDA-MB-435, SK-MEL-5, and UACC-62, respectively, from melanoma cell lines; 46% and 55% against OVCAR-3 and NCI/ADR-RES, respectively, from ovarian cancer cell lines; 41% and 52% of inhibition against A498 and CAKI-1, respectively from renal cancer; 43% of inhibition against PC-3 from prostate cancer and 42% of inhibition against MCF7 cell line from breast cancer. Compound **6f** is the second most potent compound with a mean growth inhibition percentage of 18%. **6f** exerted 40%, 46%, 44%, and 49% growth inhibition against IGROV1, A498, MCF-7, and T-47D cell lines, respectively.

2.3 | Estimation of physicochemical, pharmacokinetic, and ADME properties

Estimation of the physicochemical and pharmacokinetic properties, as well as ADME parameters of the synthesized imidazopyrimidines, was carried out using SwissADME free web tool.^[33] Selected results

TABLE 4 In vitro growth inhibition % of the selected compounds against a panel of tumor cell lines at $10 \mu\text{M}$

Subpanel	Growth inhibition %								
	6a	6b	6c	6d	6f	6g	6h	6p	9d
Leukemia									
CCRF-CEM	- ^a	-	-	-	-	-	-	-	44
HL-60(TB)	-	-	-	-	20	13	-	11	81
K-562	-	24	14	-	13	11	-	14	81
MOLT-4	-	13	-	-	-	-	-	11	60
PRMI-8226	-	-	-	-	20	-	-	-	25
SR	10	11	13	16	18	17	-	27	84
Non-small-cell lung cancer									
A549/ATTC	-	-	-	-	12	-	-	-	34
EKVX	25	24	-	-	30	-	-	-	12
HOP-62	24	39	14	19	13	-	-	13	32
HOP-92	19	35	-	-	10	-	-	17	45
NCI-H226	14	24	-	10	-	-	-	-	13
NCI-H23	23	23	-	-	26	-	12	13	28
NCI-H322M	11	-	-	-	11	-	-	-	-
NCI-H460	-	-	-	-	25	-	-	-	53
NCI-H522	23	17	20	19	34	19	21	27	64
Colon cancer									
COLO-205	-	-	-	-	-	-	-	-	23
HCC-2998	17	15	-	-	20	-	-	-	24
HCT-116	13	-	-	18	21	11	-	-	49
HCT-15	-	-	-	-	33	-	-	-	62
HT29	-	-	-	-	20	-	-	12	59
KM12	10	13	-	10	25	-	-	-	56
SW-620	-	-	-	-	-	-	-	-	60
CNS cancer									
SF-268	-	-	-	-	-	-	-	-	19
SF-295	22	17	10	-	38	-	-	15	54
SF-539	10	-	-	-	16	-	-	24	26
SNB-19	-	15	-	-	12	-	-	-	32
SNB-75	21	20	23	30	30	26	-	32	32
U251	-	11	-	-	14	-	-	-	44
Melanoma									
LOX IMVI	13	11	-	-	20	-	-	11	34
MALME-3M	-	-	19	13	20	-	-	-	22
M14	-	12	10	-	18	-	-	-	50
MDA-MB-435	-	-	-	-	-	-	-	16	lethal
SK-MEL-2	27	-	-	-	22	-	14	-	26
SK-MEL-28	-	-	-	-	14	-	10	-	27
SK-MEL-5	12	11	-	16	26	-	-	-	45
UACC-257	-	-	-	-	13	-	-	-	17
UACC-62	12	15	-	-	39	-	-	18	63
Ovarian cancer									
IGROV1	49	21	20	25	40	-	-	-	33
OVCAR-3	14	11	13	11	13	-	-	13	46
OVCAR-4	-	-	-	16	-	-	-	-	-
OVCAR-5	-	14	-	13	-	-	-	-	-
OVCAR-8	-	-	-	-	-	-	-	-	10
NCI/ADR-RES	-	-	-	-	-	-	-	-	55
SK-OV-3	23	30	13	18	26	-	-	15	18
Renal cancer									
786-0	-	-	-	-	20	-	-	11	21
A498	-	-	-	-	46	-	-	16	41
ACHN	17	14	-	-	15	-	-	13	12
CAKI-1	17	31	19	23	-	10	-	27	52
RXF 393	-	-	-	-	-	-	-	-	28
SN 12C	-	10	-	-	-	-	-	-	11
TK-10	-	-	-	-	-	-	-	-	-
UO-31	35	39	35	30	33	19	13	33	31

(Continues)

TABLE 4 (Continued)

Subpanel	Growth inhibition %								
	6a	6b	6c	6d	6f	6g	6h	6p	9d
Prostate cancer									
PC-3	25	25	-	10	32	-	-	-	43
DU-145	-	-	-	-	-	-	-	-	-
Breast cancer									
MCF7	29	20	17	26	44	-	17	13	42
MDA-MB-231/ATTC	24	28	16	-	-	-	-	12	38
HS 578T	11	16	-	-	-	-	-	10	32
BT-549	11	-	-	16	30	11	-	11	36
T-47D	28	45	23	28	49	12	-	22	26
MDA-MB-468	-	-	-	-	28	-	-	-	17

^a% of growth inhibition is <10%.

are depicted in Table 5. Analysis of the obtained results revealed that the synthesized imidazopyrimidines **6a–u** and **9a–d** have acceptable physicochemical properties such as molecular weights between 257–481 g/mol, topological polar surface areas (TPSA) ranging from 50.16 to 110.87 Å, *i*LOGP (octanol-water partition coefficient)^[34] between 2.43 and 3.63 and an acceptable number of hydrogen-bond donors and acceptors.

The imidazopyrimidines have moderate water solubility and all of them are predicted to be well absorbed from GIT. With the exception of compounds **6a–e**, **6h**, and **9a–d**, the rest of compounds do not have the probability to penetrate the blood–brain barrier; therefore, no side effects are expected to occur in the CNS. Moreover, most of the examined compounds are nonsubstrates for the most important efflux transporter P-glycoprotein, which exerts a predominate role in pumping xenobiotics outside the cells. Hence, the imidazopyrimidines are expected to be well absorbed and controlled excreted from the site of action.

Bioavailability radar provided from SwissADME web tool^[33] showed that most of the tested compounds exhibited promising predicted physicochemical properties for oral bioavailability. For instance, Figure 5 displays the bioavailability radar chart of compounds **6f**, **6g**, and **9d** (for the bioavailability radar for the rest of compounds; check Supporting Information). The ideal space of six physicochemical parameters, for example, size, polarity, lipophilicity, solubility, flexibility, and saturation for oral bioavailability are located in the pink-colored area.^[33] All the synthesized imidazopyrimidines are almost present in the pink area; the fraction of sp³ hybridized carbons is <0.25 in some cases, hence it is deviated out from the pink zone. It is interesting to mention that none of **6a–u** and **9a–d** violated the drug-likeness rules including Lipinski's rule,^[35] Veber rule,^[36] Ghose-filter,^[37] Egan,^[38] and Muegge's^[39] filter and they do not exhibit any of Pan Assay Interference subcompounds.^[40]

From results of the ADME prediction study, it was interesting to summarize that the synthesized imidazopyrimidines not only have promising chemotherapeutic properties but also satisfy the essential physicochemical, pharmacokinetic, and drug-likeness parameters for future discovery of chemotherapeutic agents.

3 | CONCLUSION

In summary, we have presented a simple and efficient method for the synthesis of a new series of imidazopyrimidines **6** and **9** by a domino reaction between 2-imino-4-oxo-6-substituted-1,2,3,4-tetrahydropyrimidines **4** or **8** and 2-bromoacetophenone **5**. The newly synthesized compounds **6** and **9** showed promising activity against Gram(–) bacteria over Gram(+) ones. Generally, compounds exhibiting a phenyl group at position-7 **6a–g** demonstrated promising antibacterial activity over compounds having methoxyphenyl groups **6i–u**. Compounds **6c**, **6f**, and **6g** showed a potent and broad spectrum of antibacterial activity over the tested microorganisms. Both **6c** and **6g** with chlorophenyl groups at position-2 showed MIC of 10.0 and 12.5 µg/ml against *E. coli* and *S. typhi*, respectively, whereas compound **6f** with 2-methoxyphenyl group at position-2 displayed MIC of 12.5, 12.5 and 25 µg/ml against *E. coli*, *P. aeruginosa* and *S. typhi*, respectively. In addition, **6f** and **6g** displayed IC₅₀ of 1.14 and 0.73 µM in GyrB ATPase assay. The synthesized compounds revealed promising antiproliferative activity against NCI cancer cell lines. Compound **9d** showed a broad spectrum of cytotoxic activity between 10% to lethal effect against the tested cell lines. In silico prediction of physicochemical and pharmacokinetic properties of the new imidazopyrimidines showed that they are promising candidates to be further optimized for the discovery of oral chemotherapeutic agents.

4 | EXPERIMENTAL

4.1 | Chemistry

4.1.1 | General remarks

All chemicals were purchased from commercial suppliers. Analytical thin-layer chromatography was performed on precoated silica gel 60 F₂₄₅ aluminum plates (Merck) with visualization under ultraviolet (UV) light. Melting points were determined on a Stuart SMP30 melting point apparatus with open capillary tubes and are uncorrected. Elemental analysis and spectral data analysis of the compounds were performed in the Microanalytical Labs, National Research Centre, Cairo, Egypt. Infrared (IR) spectra (4,000–400 cm⁻¹) were recorded using KBr pellets in a Jasco FT/IR 6100E Fourier transform infrared spectrophotometer. ¹H-NMR and ¹³C-NMR spectra were recorded at 400 (100) and 300 (75) MHz on Bruker, Agilent and a Varian Unity Inova instrument, respectively, using dimethyl sulfoxide (DMSO)-*d*₆ as a solvent. Chemical shifts are given in parts per million (ppm) relative to tetramethylsilane as internal standards. Coupling constants are reported in Hertz (Hz).

The original spectra of the investigated compounds are provided as Supporting Information, as are their InChI codes together with some biological activity data.

TABLE 5 Selected calculated physicochemical and pharmacokinetic properties of 6a-u and 9a-d from SwissADME free web tool

Product	MW	Rotatable bonds	H-bond Acc.	H-bond Don.	MR	TPSA	Log P	GI absorption	BBB permeant	Pgp substrate
6a	312.32	2	3	1	91.4	73.95	2.51	High	Yes	No
6b	330.32	2	4	1	91.36	73.95	2.56	High	Yes	No
6c	346.77	2	3	1	96.41	73.95	2.72	High	Yes	No
6d	391.22	2	3	1	99.1	73.95	2.84	High	Yes	No
6e	326.35	2	3	1	96.37	73.95	2.79	High	Yes	No
6f	342.35	3	4	1	97.89	83.18	2.9	High	No	No
6g	381.21	2	3	1	101.42	73.95	2.88	High	No	No
6h	362.38	2	3	1	108.91	73.95	2.91	High	Yes	Yes
6i	360.34	3	5	1	97.85	83.18	2.95	High	No	No
6j	376.8	3	4	1	102.9	83.18	3.07	High	No	No
6k	372.38	4	5	1	104.38	92.41	3.1	High	No	No
6l	390.37	4	6	1	104.34	92.41	3.13	High	No	No
6m	406.82	4	5	1	109.39	92.41	3.32	High	No	No
6n	402.4	5	6	1	110.88	101.64	3.31	High	No	Yes
6o	402.4	5	6	1	110.88	101.64	3.19	High	No	Yes
6p	436.85	5	6	1	115.89	101.64	3.41	High	No	No
6q	481.3	5	6	1	118.58	101.64	3.56	High	No	No
6r	416.43	5	6	1	115.84	101.64	3.43	High	No	Yes
6s	432.43	6	7	1	117.37	110.87	3.63	High	No	Yes
6t	471.29	5	6	1	120.9	101.64	3.49	High	No	No
6u	452.46	5	6	1	128.38	101.64	3.53	High	No	Yes
9a	259.69	1	2	1	71.22	50.16	2.43	High	Yes	No
9b	257.26	2	3	1	70.98	50.16	2.53	High	Yes	No
9c	273.72	2	2	1	76.03	50.16	2.7	High	Yes	No
9d	305.31	2	3	1	86.64	50.16	2.76	High	Yes	No

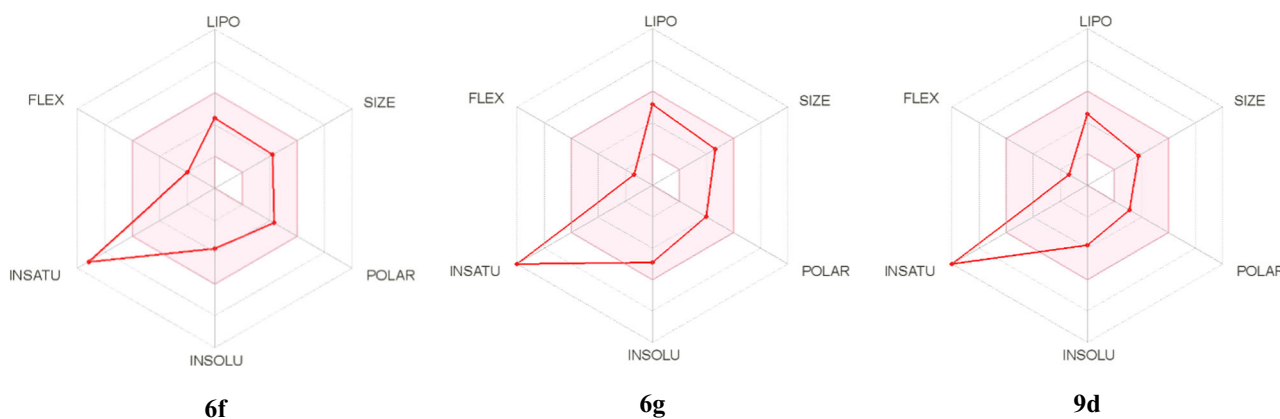
Abbreviations: ADME, absorption, distribution, metabolism, and excretion; BBB, blood-brain barrier; GI, gastrointestinal; MR: molecular refractivity; MW, molecular weights; Pgp, p-glycoprotein; TPSA, topological polar surface areas.

4.1.2 | Synthesis of 4a-d and 8a-c

The starting 2-imino-4-oxo-6-substituted-1,2,3,4-tetrahydropyrimidine-5-carbonitriles **4** and 2-imino-6-substituted-2,3-dihydropyrimidin-4(1H)-ones **8** were synthesized according to the previously reported procedure.^[21,28]

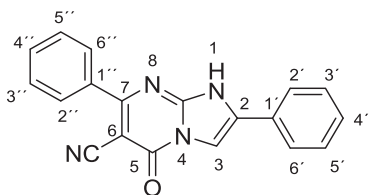
4.1.3 | General procedure for the synthesis of 6a-u and 9a-d

A mixture of equivalent amounts of **4** or **8**, 2-bromoacetophenones **5** and NaHCO₃ was stirred in ethanol under reflux for 4 hr. The reaction mixture was then cooled to room temperature followed by

**FIGURE 5** Bioavailability radar plot from SwissADME online web tool for 6f, 6g, and 9d

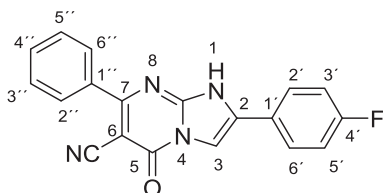
filtration and the filter was washed with ethanol. The filtrate was concentrated to one-third its original volume and poured on to ice/water and neutralized with 2N HCl. The precipitated product was filtered and dried to give the crude product, which was further purified by crystallization from methanol or by column chromatography to give analytically pure products.

5-Oxo-2,7-diphenyl-1,5-dihydroimidazo[1,2-a]pyrimidine-6-carbonitrile (6a)



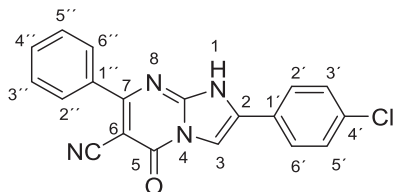
White powder; yield: 56%; mp >300°C; $^1\text{H-NMR}$ (400 MHz; DMSO- d_6) 7.42–7.46 (1H, m, H-4'), 7.49–7.53 (2H, m, H-3', H-5'), 7.55–7.57 (3H, m, H-3', H-4', H-5'), 7.86–7.88 (2H, m, H-2', H-6' or H-2'', H-6''), 8.00 (2H, d, $^3J=7.2$ Hz, H-2', H-6' or H-2'', H-6''), and 8.42 ppm (1H, s, H-3); $^{13}\text{C-NMR}$ (100 MHz; DMSO- d_6) 82.91, 104.55, 117.50, 125.47, 127.04, 128.39, 128.50, 129.16, 129.50, 130.69, 131.58, 136.84, 147.14, 156.53, and 166.52 ppm; Anal. calcd. for $\text{C}_{19}\text{H}_{12}\text{N}_4\text{O}$: C, 73.07; H, 3.87; N, 17.94. Found: C, 73.35; H, 3.48; N, 17.63.

2-(4-Fluorophenyl)-5-oxo-7-phenyl-1,5-dihydroimidazo[1,2-a]pyrimidine-6-carbonitrile (6b)



White powder; yield: 54%; mp, >300°C; $^1\text{H-NMR}$ (400 MHz; DMSO- d_6) 7.38 (2H, t, $^3J=8.8$ Hz, H-3', H-5'), 7.56–7.57 (3H, m, H-3'', H-4'', H-5''), 7.86–7.88 (2H, m, H-2', H-6'), 8.00–8.03 (2H, m, H-2'', H-6''), 8.43 (1H, s, H-3), and 14.27 ppm (1H, br., NH); Anal. calcd. for $\text{C}_{19}\text{H}_{11}\text{FN}_4\text{O}$: C, 69.09; H, 3.36; N, 16.96. Found: C, 69.39; H, 3.12; N, 16.60.

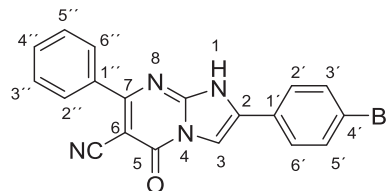
2-(4-Chlorophenyl)-5-oxo-7-phenyl-1,5-dihydroimidazo[1,2-a]pyrimidine-6-carbonitrile (6c)



White powder; yield: 50%; mp, >300°C; ν max (atr) cm^{-1} 3,137, 2,214, 1,654, 1,578, and 1,484; $^1\text{H-NMR}$ (400 MHz; DMSO- d_6) 7.56–7.59 (5H, m, H-2', H-3'', H-4'', H-5'', H-6''), 7.86 (2H, d, $^3J=6.8$ Hz, H-2', H-6'), 7.98 (2H, d, $^3J=6.8$ Hz, H-3', H-5'), and 8.47 ppm (1H, s, H-3); $^{13}\text{C-NMR}$

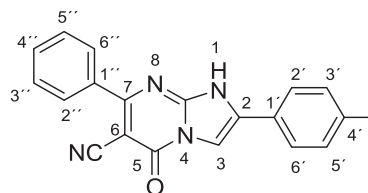
(100 MHz; DMSO- d_6) 82.14, 105.02, 113.23, 117.65, 127.22, 128.20, 128.38, 128.49, 129.20, 130.63, 133.89, 135.38, 147.45, 154.46, and 166.60 ppm; Anal. calcd. for $\text{C}_{19}\text{H}_{11}\text{ClN}_4\text{O}$: C, 65.81; H, 3.20; N, 16.16. Found: C, 65.58; H, 3.55; N, 16.03.

2-(4-Bromophenyl)-5-oxo-7-phenyl-1,5-dihydroimidazo[1,2-a]pyrimidine-6-carbonitrile (6d)



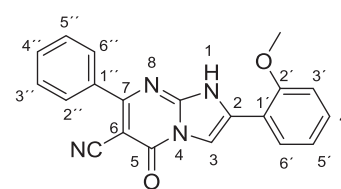
White powder; yield: 56%; mp, >300°C; ν max (atr) cm^{-1} 3,200, 3,056, 2,220, 1,652, 1,575, and 1,482; $^1\text{H-NMR}$ (400 MHz; DMSO- d_6) 7.49–7.57 (3H, m, H-3'', H-4'', H-5''), 7.72 (2H, d, $^3J=7.5$ Hz, H-2', H-6'), 7.85–7.86 (2H, m, H-2', H-6'), 7.92 (2H, d, $^3J=7.6$ Hz, H-3', H-5'), and 8.49 ppm (1H, s, H-3); $^{13}\text{C-NMR}$ (100 MHz; DMSO- d_6) 82.71, 105.14, 113.33, 117.50, 122.66, 127.45, 128.40, 128.49, 130.69, 131.01, 132.13, 135.41, 147.16, 156.59, and 165.45 ppm; Anal. calcd. for $\text{C}_{19}\text{H}_{11}\text{BrN}_4\text{O}$: C, 58.33; H, 2.83; N, 14.32. Found: C, 58.71; H, 2.53; N, 14.64.

5-Oxo-7-phenyl-2-(p-tolyl)-1,5-dihydroimidazo[1,2-a]pyrimidine-6-carbonitrile (6e)



White powder; yield: 39%; mp, >300°C; ν max (atr) cm^{-1} 3,300, 3,118, 2,217, 1,646, 1,562, and 1,480; $^1\text{H-NMR}$ (400 MHz; DMSO- d_6) 2.32 (3H, s, CH₃), 7.27 (2H, d, $^3J=7.8$ Hz, H-3', H-5'), 7.54–7.55 (3H, m, H-3'', H-4'', H-5''), 7.79 (2H, d, $^3J=7.8$ Hz, H-2', H-6'), 7.84 (2H, d, $^3J=7.1$ Hz, H-2'', H-6''), and 8.27 ppm (1H, s, H-3); $^{13}\text{C-NMR}$ (100 MHz; DMSO- d_6) 20.91, 82.72, 103.89, 117.59, 124.36, 125.42, 128.38, 128.49, 129.70, 130.63, 131.88, 136.93, 139.23, 147.13, 156.57, and 166.30 ppm; Anal. calcd. for $\text{C}_{20}\text{H}_{14}\text{N}_4\text{O}$: C, 73.61; H, 4.32; N, 17.17. Found: C, 73.37; H, 4.11; N, 17.45.

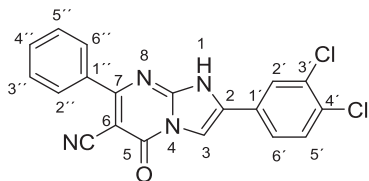
2-(2-Methoxyphenyl)-5-oxo-7-phenyl-1,5-dihydroimidazo[1,2-a]pyrimidine-6-carbonitrile (6f)



White powder; yield: 66%; mp, >300°C; $^1\text{H-NMR}$ (400 MHz; DMSO- d_6) 3.99 (3H, s, OCH₃), 7.11 (1H, t, $^3J=7.6$ Hz, H-5'), 7.28 (1H, d, $^3J=8.4$ Hz,

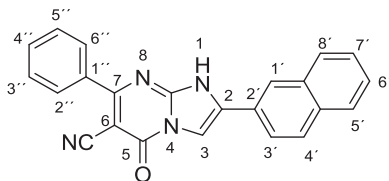
H-3'), 7.46 (1H, t, $^3J = 8.4$ Hz, H-4'), 7.55–7.57 (3H, m, H-3'', H-4'', H-5''), 7.85–7.89 (3H, m, H-2'', H-6'', H-6'), and 8.02 ppm (1H, s, H-3); $^{13}\text{C-NMR}$ (100 MHz; DMSO- d_6) 55.82, 82.77, 106.42, 111.99, 115.17, 117.53, 120.83, 127.24, 128.37, 128.52, 129.63, 130.66, 130.87, 136.89, 146.47, 156.50, 156.53, and 166.58 ppm; Anal. calcd. for $\text{C}_{20}\text{H}_{14}\text{N}_4\text{O}_2$: C, 70.17; H, 4.12; N, 16.37. Found: C, 70.38; H, 4.45; N, 16.08.

2-(3,4-Dichlorophenyl)-5-oxo-7-phenyl-1,5-dihydroimidazo[1,2-a]pyrimidine-6-carbonitrile (**6g**)



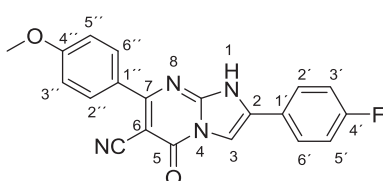
White powder; yield: 39%; mp, $>300^\circ\text{C}$; ν max (atr) cm^{-1} 3,400, 3,122, 2,213, 1,692, 1,589, and 1,491; $^1\text{H-NMR}$ (400 MHz; DMSO- d_6) 7.55–7.57 (3H, m, H-3'', H-4'', H-5''), 7.77 (1H, d, $^3J = 8.4$ Hz, H-5'), 7.84–7.87 (2H, m, H-2'', H-6''), 7.93 (1H, dd, $^3J = 8.4$ Hz, d, $^4J = 2.0$ Hz, H-6'), 8.27 (1H, d, $^4J = 2.0$ Hz, H-2'), and 8.58 ppm (1H, s, H-3); $^{13}\text{C-NMR}$ (100 MHz; DMSO- d_6) 82.61, 106.14, 117.45, 125.50, 127.26, 128.24, 128.45, 128.53, 128.65, 130.80, 131.39, 131.78, 132.15, 136.65, 147.23, 156.56, and 166.44 ppm; Anal. calcd. for $\text{C}_{19}\text{H}_{10}\text{Cl}_2\text{N}_4\text{O}$: C, 59.86; H, 2.64; N, 14.70. Found: C, 59.54; H, 2.33; N, 14.92.

2-(Naphthalen-2-yl)-5-oxo-7-phenyl-1,5-dihydroimidazo[1,2-a]pyrimidine-6-carbonitrile (**6h**)



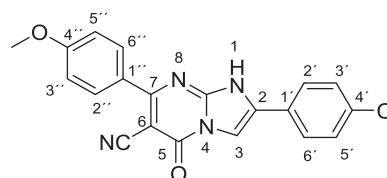
White powder; yield: 75%; mp, $>300^\circ\text{C}$; $^1\text{H-NMR}$ (400 MHz; DMSO- d_6) 7.57–7.59 (5H, m, H-2'', H-3'', H-4'', H-5'', H-6''), 7.87–7.96 (4H, m, H-5', H-6', H-7', H-8'), 8.03 (1H, d, $^3J = 8.4$ Hz, H-4'), 8.09 (1H, dd, $^3J = 8.8$ Hz, $^4J = 1.6$ Hz, H-3'), 8.50 (1H, s, H-3 or H-1'), and 8.52 ppm (1H, s, H-3 or H-1'); $^{13}\text{C-NMR}$ (100 MHz; DMSO- d_6) 82.89, 105.07, 117.52, 123.05, 124.51, 124.57, 127.09, 127.11, 127.78, 128.15, 128.40, 128.51, 128.84, 130.69, 131.76, 132.70, 132.98, 136.86, 147.25, 156.54, and 166.48 ppm; Anal. calcd. for $\text{C}_{23}\text{H}_{14}\text{N}_4\text{O}$: C, 76.23; H, 3.89; N, 15.46. Found: C, 76.53; H, 3.65; N, 15.78.

2-(4-Fluorophenyl)-7-(4-methoxyphenyl)-5-oxo-1,5-dihydroimidazo[1,2-a]pyrimidine-6-carbonitrile (**6i**)



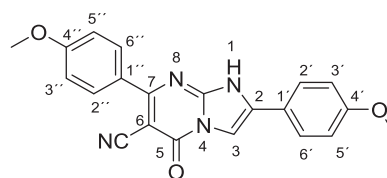
Pale yellow powder; yield: 43%; mp, $>300^\circ\text{C}$; ν max (atr) cm^{-1} 3,379, 3,145, 3,005, 2,218, 1,678, 1,566, and 1,489; $^1\text{H-NMR}$ (400 MHz; DMSO- d_6) 3.80 (3H, s, OCH_3), 7.03 (2H, d, $^3J = 8.8$ Hz, H-3'', H-5''), 7.60 (2H, dd, $J = 8.4$ Hz, $J = 5.6$ Hz, H-3', H-5'), 7.86 (2H, d, $J = 9.0$ Hz, H-2'', H-6''), 8.13 (2H, dd, $J = 8.8$ Hz, $J = 5.6$ Hz, H-2', H-6'), and 8.18 ppm (1H, s, H-3); Anal. calcd. for $\text{C}_{20}\text{H}_{13}\text{FN}_4\text{O}_2$: C, 66.66; H, 3.64; N, 15.55. Found: C, 66.42; H, 3.43; N, 15.87.

2-(4-Chlorophenyl)-7-(4-methoxyphenyl)-5-oxo-1,5-dihydroimidazo[1,2-a]pyrimidine-6-carbonitrile (**6j**)



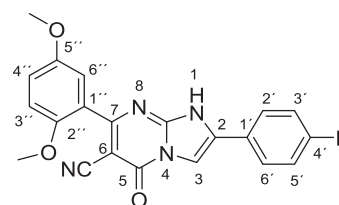
Pale yellow powder; yield: 42%; mp, $>300^\circ\text{C}$; $^1\text{H-NMR}$ (400 MHz; DMSO- d_6) 3.83 (3H, s, OCH_3), 7.09 (2H, d, $^3J = 8.8$ Hz, H-3'', H-5''), 7.54 (2H, d, $^3J = 8.4$ Hz, H-2'', H-6''), 7.87 (2H, d, $^3J = 8.4$ Hz, H-2', H-6'), 7.92 (2H, d, $^3J = 8.4$ Hz, H-3', H-5'), and 8.37 ppm (1H, s, H-3); $^{13}\text{C-NMR}$ (100 MHz; DMSO- d_6) 55.42, 82.73, 99.59, 111.12, 113.81, 114.69, 127.18, 128.80, 129.23, 130.17, 130.32, 130.79, 134.00, 147.01, 159.63, and 161.32 ppm; Anal. calcd. for $\text{C}_{20}\text{H}_{13}\text{ClN}_4\text{O}_2$: C, 63.75; H, 3.48; N, 14.87. Found: C, 63.48; H, 3.75; N, 14.51.

2,7-Bis(4-methoxyphenyl)-5-oxo-1,5-dihydroimidazo[1,2-a]pyrimidine-6-carbonitrile (**6k**)



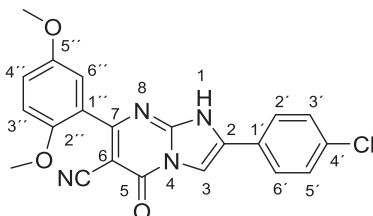
Pale yellow powder; yield: 33%; mp, $>300^\circ\text{C}$; $^1\text{H-NMR}$ (400 MHz; DMSO- d_6) 3.80 (3H, s, OCH_3), 3.84 (3H, s, OCH_3), 7.05 (2H, d, $^3J = 8.8$ Hz, H-3'', H-5''), 7.10 (2H, d, $^3J = 8.8$ Hz, H-3', H-5'), 7.88 (2H, ov. d-like, $^3J = 8.8$ Hz, H-2'', H-6'' or H-2', H-6'), 7.89 (2H, ov. d-like, $^3J = 8.4$ Hz, H-2'', H-6'' or H-2', H-6'), 8.24 (1H, s, H-3), and 13.93 ppm (1H, br., NH); $^{13}\text{C-NMR}$ (100 MHz; DMSO- d_6) 55.80, 56.01, 82.65, 106.27, 111.95, 117.72, 120.81, 125.40, 127.17, 130.85, 131.31, 132.10, 139.52, 146.18, 155.48, 156.52, and 165.94 ppm; Anal. calcd. for $\text{C}_{21}\text{H}_{16}\text{N}_4\text{O}_3$: C, 67.73; H, 4.33; N, 15.05. Found: C, 67.43; H, 4.65; N, 15.35.

7-(2,5-Dimethoxyphenyl)-2-(4-fluorophenyl)-5-oxo-1,5-dihydroimidazo[1,2-a]pyrimidine-6-carbonitrile (**6l**)



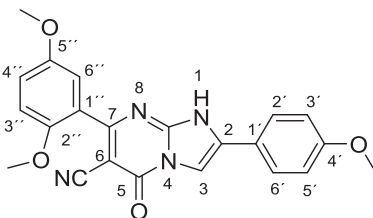
Pale yellow powder; yield: 25%; mp, >300°C; ¹H-NMR (400 MHz; DMSO-*d*₆) 3.74 (3H, s, OCH₃), 3.77 (3H, s, OCH₃), 6.98 (1H, d, ⁴J = 3.2 Hz, H-6''), 7.07 (1H, dd, ³J = 8.8 Hz, ⁴J = 3.2 Hz, H-4''), 7.12 (1H, d, ³J = 9.0 Hz, H-3''), 7.37 (2H, t, ³J = 8.8 Hz, H-3', H-5'), 7.99–8.02 (2H, m, H-2', H-6'), 8.43 (1H, s, H-3), and 14.26 ppm (1H, br., NH); ¹³C-NMR (100 MHz; DMSO-*d*₆) 55.64, 55.97, 85.83, 104.55, 113.17, 115.05, 116.33 (d, *J* = 21.8 Hz), 116.76 (d, *J* = 21.2 Hz), 124.06, 126.83, 127.98 (d, *J* = 8.6 Hz), 131.36, 147.12, 150.42, 152.86, 154.23, 155.89, 162.69 (d, *J* = 245.6 Hz), and 165.15 ppm; Anal. calcd. for C₂₁H₁₅FN₄O₃: C, 64.61; H, 3.87; N, 14.35. Found: C, 64.92; H, 3.65; N, 14.68.

2-(4-Chlorophenyl)-7-(2,5-dimethoxyphenyl)-5-oxo-1,5-dihydroimidazo[1,2-*a*]pyrimidine-6-carbonitrile (6m)



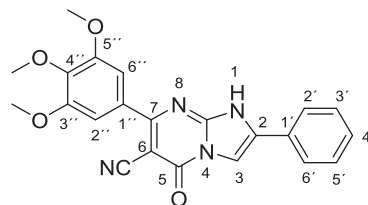
Pale yellow powder; yield: 46%; mp, >300°C; ν max (atr) cm⁻¹ 3,475, 3,136, 3,044, 2,222, 1,663, 1,578, and 1,489; ¹H-NMR (400 MHz; DMSO-*d*₆) 3.74 (3H, s, OCH₃), 3.77 (3H, s, OCH₃), 6.98 (1H, d, ⁴J = 3.2 Hz, H-6''), 7.07 (1H, d, ³J = 9.2 Hz, ⁴J = 3.2 Hz, H-4''), 7.12 (1H, d, ³J = 9.2 Hz, H-3''), 7.58 (2H, d, ³J = 8.4 Hz, H-2', H-6'), 7.97 (2H, d, ³J = 8.4 Hz, H-3', H-5'), 8.48 (1H, s, H-3), and 14.24 ppm (1H, br., NH); ¹³C-NMR (100 MHz; DMSO-*d*₆) 55.58, 55.91, 82.41, 105.13, 113.10, 114.98, 115.88, 116.57, 116.81, 127.28, 129.21, 129.65, 133.95, 147.15, 150.36, 152.78, 155.84, 156.60, and 164.50 ppm; Anal. calcd. for C₂₁H₁₅ClN₄O₃: C, 62.00; H, 3.72; N, 13.77. Found: C, 62.32; H, 3.93; N, 13.90.

7-(2,5-Dimethoxyphenyl)-2-(4-methoxyphenyl)-5-oxo-1,5-dihydroimidazo[1,2-*a*]pyrimidine-6-carbonitrile (6n)



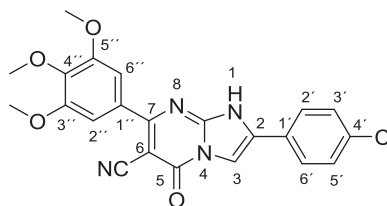
Pale yellow powder; yield: 37%; mp, >300°C; ¹H-NMR (400 MHz; DMSO-*d*₆) 3.74 (3H, s, OCH₃), 3.77 (3H, s, OCH₃), 3.81 (3H, s, OCH₃), 6.98 (1H, d, ⁴J = 2.8 Hz, H-6''), 7.06–7.08 (3H, m, H-4', H-3', H-5'), 7.12 (1H, d, ³J = 9.1 Hz, H-3''), 7.89 (2H, d, ³J = 8.8 Hz, H-2', H-6'), 8.30 (1H, s, H-3), and 14.12 ppm (1H, br., NH); ¹³C-NMR (100 MHz; DMSO-*d*₆) 55.47, 55.98, 56.02, 82.09, 106.14, 113.17, 115.21, 116.02, 116.21, 116.36, 116.43, 122.31, 126.79, 131.59, 132.99, 146.33, 150.27, 152.75, 155.35, and 165.73 ppm; Anal. calcd. for C₂₂H₁₈N₄O₄: C, 65.66; H, 4.51; N, 13.92. Found: C, 65.41; H, 4.88; N, 13.65.

5-Oxo-2-phenyl-7-(3,4,5-trimethoxyphenyl)-1,5-dihydroimidazo[1,2-*a*]pyrimidine-6-carbonitrile (6o)



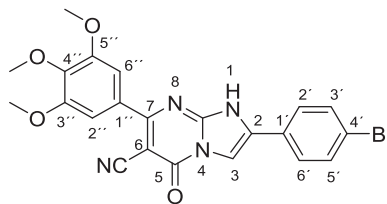
White powder; yield: 66%; mp, >300°C; ¹H-NMR (400 MHz; DMSO-*d*₆) 3.76 (3H, s, OCH₃), 3.84 (6H, s, OCH₃), 7.23 (2H, s, H-2', H-6''), 7.42–7.52 (3H, m, H-3', H-4', H-5'), 7.95 (2H, d, ³J = 7.6 Hz, H-2', H-6'), and 8.40 ppm (1H, s, H-3); ¹³C-NMR (100 MHz; DMSO-*d*₆) 56.04, 60.23, 82.73, 104.55, 106.29, 117.77, 125.48, 127.04, 129.18, 129.53, 131.67, 131.80, 139.58, 146.98, 152.53, 156.58, and 165.89 ppm; Anal. calcd. for C₂₂H₁₈N₄O₄: C, 65.66; H, 4.51; N, 13.92. Found: C, 65.34; H, 4.31; N, 13.71.

2-(4-Chlorophenyl)-5-oxo-7-(3,4,5-trimethoxyphenyl)-1,5-dihydroimidazo[1,2-*a*]pyrimidine-6-carbonitrile (6p)



White powder; yield: 72%; mp, >300°C; ¹H-NMR (300 MHz; DMSO-*d*₆) 3.76 (3H, s, OCH₃), 3.85 (6H, s, OCH₃), 7.23 (2H, s, H-2', H-6''), 7.59 (2H, d, ³J = 8.7 Hz, H-2', H-6'), 7.99 (2H, d, ³J = 8.4 Hz, H-3', H-5'), 8.49 (1H, s, H-3), and 14.29 ppm (1H, br., NH); ¹³C-NMR (75 MHz; DMSO-*d*₆) 56.00, 60.18, 82.64, 105.12, 106.24, 117.69, 126.20, 127.18, 129.20, 130.77, 131.68, 134.01, 139.56, 146.99, 152.49, 156.53, and 165.82 ppm; Anal. calcd. for C₂₂H₁₇ClN₄O₄: C, 60.49; H, 3.92; N, 12.83. Found: C, 60.17; H, 3.67; N, 12.54.

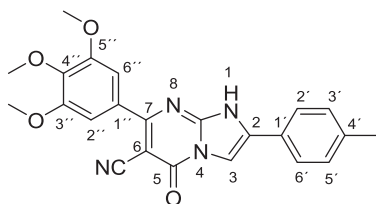
2-(4-Bromophenyl)-5-oxo-7-(3,4,5-trimethoxyphenyl)-1,5-dihydroimidazo[1,2-*a*]pyrimidine-6-carbonitrile (6q)



White powder; yield: 76%; mp, 295–297°C; ν max (atr) cm⁻¹ 3,200, 3,111, 2,215, 1,660, 1,575, and 1,486; ¹H-NMR (400 MHz; DMSO-*d*₆) 3.76 (3H, s, OCH₃), 3.84 (6H, s, OCH₃), 7.22 (2H, s, H-2', H-6''), 7.59 (2H, d, ³J = 8.8 Hz, H-2', H-6'), 7.99 (2H, d, ³J = 8.8 Hz, H-3', H-5'), and 8.48 ppm (1H, s, H-3); ¹³C-NMR (100 MHz; DMSO-*d*₆) 56.01, 60.19, 82.64, 105.13, 106.25, 117.71, 126.21, 127.20, 128.96, 129.22,

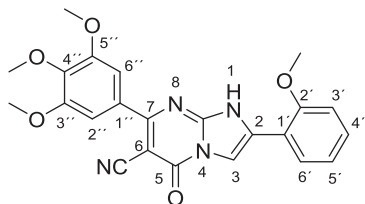
131.69, 134.03, 139.57, 147.01, 152.50, 156.55, and 165.40 ppm; Anal. calcd. for $C_{22}H_{17}BrN_4O_4$: C, 54.90; H, 3.56; N, 11.64. Found: C, 54.71; H, 3.23; N, 11.35.

5-Oxo-2-(*p*-tolyl)-7-(3,4,5-trimethoxyphenyl)-1,5-dihydroimidazo[1,2-*a*]pyrimidine-6-carbonitrile (**6r**)



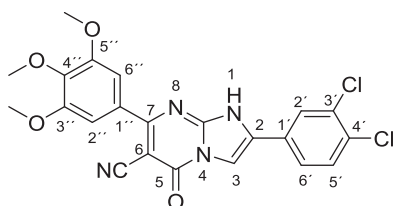
White powder; yield: 64%; mp, >300°C; $^1\text{H-NMR}$ (400 MHz; $\text{DMSO-}d_6$) 2.33 (3H, s, CH_3), 3.75 (3H, s, OCH_3), 3.84 (6H, s, OCH_3), 7.21 (2H, s, H-2', H-6'), 7.46 (2H, d, $^3J=8.4$ Hz, H-3', H-5'), 7.92 (2H, d, $^3J=8.8$ Hz, H-2', H-6'), and 8.10 ppm (1H, s, H-3); $^{13}\text{C-NMR}$ (100 MHz; $\text{DMSO-}d_6$) 20.88, 55.96, 60.16, 95.03, 103.29, 104.22, 106.17, 118.68, 125.30, 126.88, 128.69, 129.50, 132.12, 139.12, 152.40, 157.06, 157.39, and 164.24 ppm; Anal. calcd. for $C_{23}H_{20}N_4O_4$: C, 66.34; H, 4.84; N, 13.45. Found: C, 66.01; H, 4.54; N, 13.12.

2-(2-Methoxyphenyl)-5-oxo-7-(3,4,5-trimethoxyphenyl)-1,5-dihydroimidazo[1,2-*a*]pyrimidine-6-carbonitrile (**6s**)



White powder; yield: 61%; mp, >300°C; ν max (atr) cm^{-1} 3,400, 3,120, 2,942, 2,214, 1,671, 1,594, and 1,492; $^1\text{H-NMR}$ (300 MHz; $\text{DMSO-}d_6$) 3.76 (3H, s, OCH_3), 3.85 (6H, s, OCH_3), 3.99 (3H, s, OCH_3), 7.11 (1H, t, $^3J=7.2$ Hz), 7.22–7.24 (3H, m), 7.46 (1H, t, $^3J=7.2$ Hz), 7.91 (1H, d, $^3J=7.8$ Hz), 8.02 (1H, s, H-3), and 14.01 ppm (1H, br., NH); $^{13}\text{C-NMR}$ (75 MHz; $\text{DMSO-}d_6$) 55.80, 56.00, 60.17, 82.54, 106.26, 106.42, 111.96, 115.15, 117.76, 120.80, 127.19, 130.82, 131.84, 139.50, 146.29, 152.47, 156.52, and 165.94 ppm; Anal. calcd. for $C_{23}H_{20}N_4O_5$: C, 63.88; H, 4.66; N, 12.96. Found: C, 63.64; H, 4.92; N, 12.72.

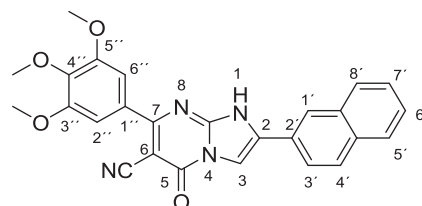
2-(3,4-Dichlorophenyl)-5-oxo-7-(3,4,5-trimethoxyphenyl)-1,5-dihydroimidazo[1,2-*a*]pyrimidine-6-carbonitrile (**6t**)



White powder; yield: 73%; mp, 198–200°C; ν max (atr) cm^{-1} 3,300, 3,117, 2,942, 2,208, 1,661, 1,592, and 1,478; $^1\text{H-NMR}$

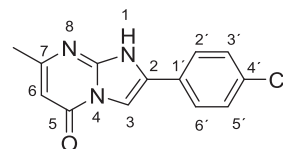
(400 MHz; $\text{DMSO-}d_6$) 3.76 (3H, s, OCH_3), 3.85 (6H, s, OCH_3), 7.22 (2H, s, H-2', H-6'), 7.79 (1H, d, $^3J=8.4$ Hz, H-5'), 7.96 (1H, dd, $^3J=8.4$ Hz, $^4J=2.1$ Hz, H-6'), 8.30 (1H, d, $^4J=1.8$ Hz, H-2'), and 8.60 ppm (1H, s, H-3); $^{13}\text{C-NMR}$ (100 MHz; $\text{DMSO-}d_6$) 56.02, 60.20, 82.65, 106.14, 106.27, 117.64, 125.43, 127.22, 129.89, 131.35, 131.76, 132.12, 134.34, 139.63, 146.99, 152.51, 156.52, 161.97, and 165.71 ppm; Anal. calcd. for $C_{22}H_{16}Cl_2N_4O_4$: C, 56.07; H, 3.42; N, 11.89. Found: C, 56.33; H, 3.76; N, 11.60.

2-(Naphthalen-2-yl)-5-oxo-7-(3,4,5-trimethoxyphenyl)-1,5-dihydroimidazo[1,2-*a*]pyrimidine-6-carbonitrile (**6u**)



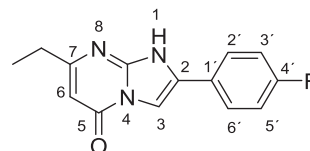
White powder; yield: 60%; mp, >300°C; $^1\text{H-NMR}$ (400 MHz; $\text{DMSO-}d_6$) 3.77 (3H, s, OCH_3), 3.86 (6H, s, OCH_3), 7.25 (2H, s, H-2', H-6'), 7.56–7.60 (2H, m), 7.91–7.99 (3H, m), 8.11–8.12 (1H, m), 8.54 (1H, s, H-3 or H-1'), 8.55 (1H, s, H-3 or H-1'), and 14.38 ppm (1H, br., NH); Anal. calcd. for $C_{26}H_{20}N_4O_4$: C, 69.02; H, 4.46; N, 12.38. Found: C, 69.38; H, 4.65; N, 12.05.

2-(4-Chlorophenyl)-7-methylimidazo[1,2-*a*]pyrimidin-5(1H)-one (**9a**)

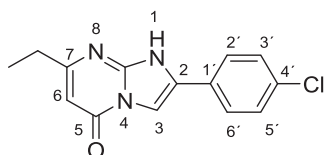


White powder; yield: 48%; mp, >300°C; ν max (atr) cm^{-1} 3,310, 2,960, 1,675, 1,563, and 1,479; $^1\text{H-NMR}$ (400 MHz; $\text{DMSO-}d_6$) 2.29 (3H, s, CH_3), 5.47 (1H, s, H-6), 7.42 (2H, d, $^3J=8.4$ Hz, H-2', H-6'), 7.90 (2H, d, $^3J=8.4$ Hz, H-3', H-5'), and 7.97 ppm (1H, s, H-3); $^{13}\text{C-NMR}$ (100 MHz; $\text{DMSO-}d_6$) 21.14, 93.43, 103.06, 126.75, 128.52, 131.50, 132.69, 137.97, 147.15, 155.17, and 157.60 ppm; Anal. calcd. for $C_{13}H_{10}ClN_3O$: C, 60.13; H, 3.88; N, 16.18. Found: C, 60.37; H, 3.98; N, 16.40.

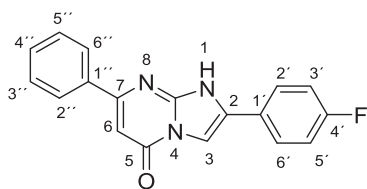
7-Ethyl-2-(4-fluorophenyl)imidazo[1,2-*a*]pyrimidin-5(1H)-one (**9b**)



White powder; yield: 48%; mp, >300°C; $^1\text{H-NMR}$ (400 MHz; $\text{DMSO-}d_6$) 1.22 (3H, t, $^3J=7.2$ Hz, CH_3), 2.57 (2H, q, $^3J=7.2$ Hz, CH_2), 5.65 (1H, s, H-6), 7.25 (2H, t, $^3J=8.8$ Hz, H-3', H-5'), 7.92–7.96 (2H, m, H-2', H-6'), and 8.10 ppm (1H, s, H-3); Anal. calcd. for $C_{14}H_{12}FN_3O$: C, 65.36; H, 4.70; N, 16.33. Found: C, 65.61; H, 4.52; N, 16.61.

2-(4-Chlorophenyl)-7-ethylimidazo[1,2-a]pyrimidin-5(1H)-one (9c)


White powder; yield: 36%; mp, >300°C; ν max (atr) cm^{-1} 3,426, 3,120, 2,928, 1,686, 1,600, 1,566, and 1,443; $^1\text{H-NMR}$ (400 MHz; $\text{DMSO-}d_6$) 1.21 (3H, t, $^3J = 7.6$ Hz, CH_3), 2.57 (2H, q, $^3J = 7.6$ Hz, CH_2), 5.65 (1H, s, H-6), 7.46 (2H, d, $^3J = 8.4$ Hz, H-2', H-6'), 7.91 (2H, d, $^3J = 8.8$ Hz, H-3', H-5'), and 8.10 ppm (1H, s, H-3); $^{13}\text{C-NMR}$ (100 MHz; $\text{DMSO-}d_6$) 12.72, 39.96, 93.75, 104.16, 126.91, 128.75, 129.21, 130.18, 130.65, 156.59, 157.34, and 168.67 ppm; Anal. calcd. for $\text{C}_{14}\text{H}_{12}\text{ClN}_3\text{O}$: C, 61.43; H, 4.42; N, 15.35. Found: C, 61.74; H, 4.71; N, 15.00.

2-(4-Fluorophenyl)-7-phenylimidazo[1,2-a]pyrimidin-5(1H)-one (9d)


White powder; yield: 33%; mp, >300°C; $^1\text{H-NMR}$ (400 MHz; $\text{DMSO-}d_6$) 5.88 (1H, s, H-6), 7.32–7.36 (3H, m, H-3'', H-4'', H-5''), 7.62 (2H, dd, $J = 8.4$ Hz, $J = 5.2$ Hz, H-3', H-5'), 7.49–7.50 (2H, m, H-2'', H-6''), 8.16 (2H, dd, $J = 8.4$ Hz, $J = 5.2$ Hz, H-2', H-6'), 8.21 (1H, s, H-3), and 13.40 ppm (1H, br., NH); Anal. calcd. for $\text{C}_{18}\text{H}_{12}\text{FN}_3\text{O}$: C, 70.81; H, 3.96; N, 13.76. Found: C, 70.58; H, 3.65; N, 13.43.

4.2 | X-ray crystallographic study

Crystals were grown following the protocol developed by Hope by dissolving the compound in CH_2Cl_2 and layering with a MeOH for liquid.^[41] Single crystal X-ray diffraction data for all compounds were collected on a Bruker APEX 2 DUO CCD diffractometer by using graphite-monochromated Mo K_α ($\lambda = 0.71073 \text{ \AA}$) radiation. Crystals were mounted on a MiTeGen MicroMount and collected at 100(2)K by using an Oxford Cryosystems Cobra low-temperature device. Data were collected by using ω and ϕ scans and were corrected for Lorentz and polarization effects by using the APEX software suite.^[42–44] Using Olex2, the structure was solved with the XT structure solution program, using the intrinsic phasing solution method and refined against $|F_2|$ with XL using least-squares minimization.^[45,46] Hydrogen atoms were generally placed in geometrically calculated positions and refined using a riding model. The phenyl ring at C7 was modeled over two positions in a 50:50% occupancy using the restraint SADI. The methoxy group at C16 were modeled over two positions in a 50:50% occupancy using the constraint EADP. Further details of data collection and

refinement can be found in Tables S1 and S2. All images were prepared by using Olex2.^[45] CCDC 1951700 contains the Supporting Information crystallographic data for this paper. These data can be obtained free of charge from The Cambridge Crystallographic Data Centre via www.ccdc.cam.ac.uk/structures.

4.3 | Biological evaluation

Antimicrobial activity and MIC of the synthesized compounds and positive control (ampicillin and levofloxacin) were evaluated by well diffusion method.^[31,32]

4.3.1 | Tested microbes

The Gram(+) bacterial strains *S. aureus* (ATCC 6538), and *B. subtilis* (ATCC 663) were used for the experiment, whereas *E. coli* (ATCC 8739), *P. aeruginosa* (ATCC 9027), *K. pneumoniae* (ATCC 10131) and *S. typhi* (ATCC 14028) were selected as Gram(−) bacterial strains for this study.

4.3.2 | Preparation of inoculums

Bacterial inoculums were prepared by growing bacteria in nutrient broth (Sigma-Aldrich) for 24 hr at 37°C. These cell suspensions were diluted with sterile nutrient broth to provide initial cell counts of about 10^4 CFU/ml.

4.3.3 | Preparation of synthetic compounds

A stock solution of 10 mg/ml in DMSO of each compound was prepared.

4.3.4 | Determination of the antibacterial activity

The well-diffusion assay was used to determine and screen the antimicrobial activity of all compounds.^[31,32] Petri dishes containing 20 ml nutrient agar culture medium at 50–70°C was left to solidify under UV light (265 nm wavelength) for 15 min. Then, they were inoculated with 0.2 ml of an overnight bacterial cell suspension matching a 0.5-McFarland standard solution. The suspension was uniformly spread using a sterile swab over the surface of the medium. Wells of 8 mm in diameter were made in the agar plates with a sterile glass Pasteur pipette and 0.1 ml of each compound of the stock solution was added into the wells. DMSO was used as a negative control, whereas ampicillin and levofloxacin (10 mg/ml) were used as positive controls. The plates were then incubated at 37°C for 24 hr. The antimicrobial activity was assayed by measuring the diameters of the inhibition zone formed around the wells in mm. Each assay was performed at least in triplicate.

4.3.5 | Determination of the minimal inhibitory concentration

Minimum inhibitory concentration studies of isolated compounds were performed according to the standard reference method for bacteria.^[31,32] The Petri dishes were inoculated with the strains as described before using the microdilution method.^[31,32] The tested compounds and the positive control (ampicillin and levofloxacin) were diluted at different concentrations ranging from 10 to 0.05 mg/ml, and each concentration was placed in a separate well. The Petri dishes were incubated for 24 hr at 37°C. The MIC was defined as the lowest concentration of the compound capable of preventing the microbial growth in the culture medium.

4.3.6 | Gyrase ATPase assay

This assay is based on the transformation of phosphoenolpyruvate to pyruvate kinase consequent with the conversion of pyruvate to lactate by lactate dehydrogenase (LDH) in the presence of NADH which is oxidized to NAD⁺. NADH absorbs strongly at 340 nm but NAD⁺ does not, enabling the reduction of NADH over time to be followed by monitoring the decrease in absorbance at 340 nm. *E. coli* gyrase for ATPase assay kit (Inspiralis) was used for testing the synthesized imidazopyrimidines **6c**, **6d**, **6f**, **6g**, and **9d**. Assays were carried out according to the manufacturer's procedure in clear colorless 96-well flat-bottomed plates with a final volume of 100 µl of the established assay buffer (50 mM Tris-HCl [pH 7.5], 1 mM ethylenediaminetetraacetic acid, 5 mM MgCl₂, 5 mM dithiothreitol, 10% [wt/vol] glycerol) containing 1 U (10 µl of 500 nM) of gyrase, 800 µM phosphoenolpyruvate, 400 µM NADH, 1.5 µl phosphokinase/LDH enzyme mix (P0294; Sigma-Aldrich), DNA and different concentrations of inhibitors. The mix was then incubated for 10 min at 25°C. Reactions were then initiated by the addition of 2 mM ATP and the decrease in absorbance at 340 nm was measured over time using an BioTek[®] Synergy HT fluorescence plate reader. IC₅₀ values were calculated using the GraphPad Prism software.^[47]

ACKNOWLEDGMENTS

The authors are grateful for the National Cancer Institute (NCI), Bethesda, MD, for performing the anticancer screening for the selected compounds over their panel of cell lines. Sincere thanks to Bioorganische Chemie, Institut für Chemie, Universität Hohenheim for running some NMR spectra. The X-ray analysis and most of the NMR measurements were supported by a grant from Science Foundation Ireland (SFI IvP 13/IA/1894).

CONFLICT OF INTERESTS

The authors declare that there are no conflicts of interests.

ORCID

Heba T. Abdel-Mohsen  <http://orcid.org/0000-0002-7610-8312>
 Amira Abood  <http://orcid.org/0000-0003-0712-9889>
 Keith J. Flanagan  <http://orcid.org/0000-0003-1656-3177>
 Mathias O. Senge  <http://orcid.org/0000-0002-7467-1654>
 Hoda I. El Diwani  <http://orcid.org/0000-0001-7525-9437>

REFERENCES

- [1] M. S. Morehead, C. Scarbrough, *Prim. Care* **2018**, 45, 467.
- [2] C. Llor, L. Bjerrum, *Ther. Adv. Drug Saf.* **2014**, 5, 229.
- [3] R. J. Fair, Y. Tor, *Perspect. Med. Chem.* **2014**, 6, 25.
- [4] R. J. Reece, A. Maxwell, *Crit. Rev. Biochem. Mol. Biol.* **1991**, 26, 335.
- [5] F. Collin, S. Karkare, A. Maxwell, *Appl. Microbiol. Biotechnol.* **2011**, 92, 479.
- [6] T. Khan, K. Sankhe, V. Suvarna, A. Sherje, K. Patel, B. Dravyakar, *Biomed. Pharmacother.* **2018**, 103, 923.
- [7] M. Oblak, M. Kotnik, T. Solmajer, *Curr. Med. Chem.* **2007**, 14, 2033.
- [8] M. Trzoss, D. C. Bensen, X. Li, Z. Chen, T. Lam, J. Zhang, C. J. Creighton, M. L. Cunningham, B. Kwan, M. Stidham, K. Nelson, V. Brown-Driver, A. Castellano, K. J. Shaw, F. C. Lightstone, S. E. Wong, T. B. Nguyen, J. Finn, L. W. Tari, *Bioorg. Med. Chem. Lett.* **2013**, 23, 1537.
- [9] L. W. Tari, M. Trzoss, D. C. Bensen, X. Li, Z. Chen, T. Lam, J. Zhang, C. J. Creighton, M. L. Cunningham, B. Kwan, M. Stidham, K. J. Shaw, F. C. Lightstone, S. E. Wong, T. B. Nguyen, J. Nix, J. Finn, *Bioorg. Med. Chem. Lett.* **2013**, 23, 1529.
- [10] J. T. Starr, R. J. Sciotti, D. L. Hanna, M. D. Huband, L. M. Mullins, H. Cai, J. W. Gage, M. Lockard, M. R. Rauckhorst, R. M. Owen, M. S. Lall, M. Tomilo, H. Chen, S. P. McCurdy, M. R. Barbachyn, *Bioorg. Med. Chem. Lett.* **2009**, 19, 5302.
- [11] P. S. Charifson, A. L. Grillot, T. H. Grossman, J. D. Parsons, M. Badia, S. Bellon, D. D. Deininger, J. E. Drumm, C. H. Gross, A. LeTiran, Y. Liao, N. Mani, D. P. Nicolau, E. Perola, S. Ronkin, D. Shannon, L. L. Swenson, Q. Tang, P. R. Tessier, S. K. Tian, M. Trudeau, T. Wang, Y. Wei, H. Zhang, D. Stamos, *J. Med. Chem.* **2008**, 51, 5243.
- [12] T. Germe, J. Voros, F. Jeannot, T. Taillier, R. A. Stavenger, E. Bacque, A. Maxwell, B. D. Bax, *Nucleic Acids Res.* **2018**, 46, 4114.
- [13] M. Gjorgjieva, T. Tomasic, M. Barancokova, S. Katsamakas, J. Ilas, P. Tammela, L. Peterlin Masic, D. Kikelj, *J. Med. Chem.* **2016**, 59, 8941.
- [14] A. Tanitame, Y. Oyamada, K. Ofuji, Y. Kyoya, K. Suzuki, H. Ito, M. Kawasaki, K. Nagai, M. Wachi, J. Yamagishi, *Bioorg. Med. Chem. Lett.* **2004**, 14, 2857.
- [15] M. Brvar, A. Perdih, M. Renko, G. Anderluh, D. Turk, T. Solmajer, *J. Med. Chem.* **2012**, 55, 6413.
- [16] M. Uria-Nickelsen, G. Neckermann, S. Sriram, B. Andrews, J. I. Manchester, D. Carcanague, S. Stokes, K. G. Hull, *Int. J. Antimicrob. Agents* **2013**, 41, 363.
- [17] R. O'Shea, H. E. Moser, *J. Med. Chem.* **2008**, 51, 2871.
- [18] C. Fitzmaurice, C. Allen, R. M. Barber, L. Barregard, Z. A. Bhutta, H. Brenner, D. J. Dicker, O. Chimed-Orchir, R. Dandona, L. Dandona, T. Fleming, M. H. Forouzanfar, J. Hancock, R. J. Hay, R. Hunter-Merrill, C. Huynh, H. D. Hosgood, C. O. Johnson, J. B. Jonas, J. Khubchandani, G. A. Kumar, M. Kutz, Q. Lan, H. J. Larson, X. Liang, S. S. Lim, A. D. Lopez, M. F. MacIntyre, L. Marczak, N. Marquez, A. H. Mokdad, C. Pinho, F. Pourmalek, J. A. Salomon, J. R. Sanabria, L. Sandar, B. Sartorius, S. M. Schwartz, K. A. Shackelford, K. Shibuya, J. Stanaway, C. Steiner, J. Sun, K. Takahashi, S. E. Vollset, T. Vos, J. A. Wagner, H. Wang, R. Westerman, H. Zeeb, L. Zoeckler, F. Abd-Allah, M. B. Ahmed, S. Alabed, N. K. Alam, S. F. Aldahri, G. Alem, M. A. Alemayohu, R. Ali, R. Al-Raddadi, A. Amare, Y. Amoako, A. Artaman,

- H. Asayesh, N. Atnafu, A. Awasthi, H. B. Saleem, A. Barac, N. Bedi, I. Bensenor, A. Berhane, E. Bernabé, B. Betsu, A. Binagwaho, D. Boneya, I. Campos-Nonato, C. Castañeda-Orjuela, F. Catalá-López, P. Chiang, C. Chibueze, A. Chitheer, J. Y. Choi, B. Cowie, S. Damte, J. das Neves, S. Dey, S. Dharmaratne, P. Dhillon, E. Ding, T. Driscoll, D. Ekwueme, A. Y. Endries, M. Farvid, F. Farzadfar, J. Fernandes, F. Fischer, T. T. G/hiwot, A. Gebru, S. Gopalani, A. Hailu, M. Horino, N. Horita, A. Hussein, I. Huybrechts, M. Inoue, F. Islami, M. Jakovljevic, S. James, M. Javanbakht, S. H. Jee, A. Kasaeian, M. S. Kadir, Y. S. Khader, Y. H. Khang, D. Kim, J. Leigh, S. Linn, R. Lunevicius, H. El Razeq, R. Malekzadeh, D. C. Malta, W. Marcenes, D. Markos, Y. A. Melaku, K. G. Meles, W. Mendoza, D. T. Mengiste, T. J. Meretoja, T. R. Miller, K. A. Mohammad, A. Mohammadi, S. Mohammed, M. Moradi-Lakeh, G. Nagel, D. Nand, Q. Le Nguyen, S. Nolte, F. A. Ogbo, K. E. Oladimeji, E. Oren, M. Pa, E. K. Park, D. M. Pereira, D. Plass, M. Qorbani, A. Radfar, A. Rafay, M. Rahman, S. M. Rana, K. Søreide, *JAMA Oncol.* **2017**, *3*, 524.
- [19] K. O. Alfarouk, C. M. Stock, S. Taylor, M. Walsh, A. K. Muddathir, D. Verduzco, A. H. Bashir, O. Y. Mohammed, G. O. Elhassan, S. Harguindey, S. J. Reshkin, M. E. Ibrahim, C. Rauch, *Cancer Cell. Int.* **2015**, *15*, 71.
- [20] H. T. Abdel-Mohsen, F. A. Ragab, M. M. Ramla, H. I. El Diwani, *Eur. J. Med. Chem.* **2010**, *45*, 2336.
- [21] H. T. Abdel-Mohsen, J. Conrad, K. Harms, D. Nohr, U. Beifuss, *RSC Adv.* **2017**, *7*, 17427.
- [22] H. T. Abdel-Mohsen, J. Conrad, U. Beifuss, *J. Org. Chem.* **2013**, *78*, 7986.
- [23] H. T. Abdel-Mohsen, A. S. Girgis, A. E. E. Mahmoud, M. M. Ali, H. I. El Diwani, *Arch. Pharm.* **2019**, *352*, e1900089.
- [24] H. T. Abdel-Mohsen, M. A. Omar, A. M. El Kerdawy, A. E. E. Mahmoud, M. M. Ali, H. I. El Diwani, *Eur. J. Med. Chem.* **2019**, *179*, 707.
- [25] M. Sahu, N. Siddiqui, *Int. J. Pharm. Pharm. Sci.* **2016**, *144*, 8.
- [26] T. H. Al-Tel, R. A. Al-Qawasmeh, *Eur. J. Med. Chem.* **2010**, *45*, 5848.
- [27] A. Kamal, G. Bharath Kumar, V. Lakshma Nayak, V. S. Reddy, A. B. Shaik, R. Rajender, M. Kashi Reddy, *MedChemComm* **2015**, *6*, 606.
- [28] H. I. El Diwani, H. T. Abdel-Mohsen, I. Salama, F. A.-F. Ragab, M. M. Ramla, S. A. Galal, M. M. Abdalla, A. Abdel-Wahab, M. A. El Demellawy, *Chem. Pharm. Bull.* **2014**, *62*, 856.
- [29] M. A. Abdullaziz, H. T. Abdel-Mohsen, A. M. El Kerdawy, F. A. F. Ragab, M. M. Ali, S. M. Abu-Bakr, A. S. Girgis, H. I. El Diwani, *Eur. J. Med. Chem.* **2017**, *136*, 315.
- [30] R. Goel, V. Luxami, K. Paul, *RSC Adv.* **2015**, *5*, 81608.
- [31] N. R. Bhalodia, V. J. Shukla, *J. Adv. Pharm. Technol. Res.* **2011**, *2*, 104.
- [32] M. A. Shakhathreh, M. L. Al-Smadi, O. F. Khabour, F. A. Shuaibu, E. I. Hussein, K. H. Alzoubi, *Drug Des. Dev. Ther.* **2016**, *10*, 3653.
- [33] A. Daina, O. Michielin, V. Zoete, *Sci. Rep.* **2017**, *7*, 42717.
- [34] A. Daina, O. Michielin, V. Zoete, *J. Chem. Inf. Model.* **2014**, *54*, 3284.
- [35] C. A. Lipinski, F. Lombardo, B. W. Dominy, P. J. Feeney, *Adv. Drug Deliv. Rev.* **2001**, *46*, 3.
- [36] D. F. Veber, S. R. Johnson, H. Y. Cheng, B. R. Smith, K. W. Ward, K. D. Kopple, *J. Med. Chem.* **2002**, *45*, 2615.
- [37] A. K. Ghose, V. N. Viswanadhan, J. J. Wendoloski, *J. Comb. Chem.* **1999**, *1*, 55.
- [38] W. J. Egan, K. M. Merz Jr., J. J. Baldwin, *J. Med. Chem.* **2000**, *43*, 3867.
- [39] I. Muegge, S. L. Heald, D. Brittelli, *J. Med. Chem.* **2001**, *44*, 1841.
- [40] J. B. Baell, G. A. Holloway, *J. Med. Chem.* **2010**, *53*, 2719.
- [41] H. Hope *Progress in Inorganic Chemistry* (Ed: K. D. Karlin), John Wiley & Sons, Hoboken **2007**, pp. 1-19.
- [42] *Saint, Version 8.37a*, Bruker AXS, Madison **2013**.
- [43] *SADABS, Version 2016/2*, Bruker AXS, Madison **2014**.
- [44] *APEX3, Version 2016.9-0*, Bruker AXS, Madison **2016**.
- [45] O. V. Dolomanov, L. J. Bourhis, R. J. Gildea, J. A. K. Howard, H. Puschmann, *J. Appl. Crystallogr.* **2009**, *42*, 339.
- [46] G. Sheldrick, *Acta Cryst. Sect. A* **2015**, *71*, 3.
- [47] J. G. Heddl, T. Lu, X. Zhao, K. Drlica, A. Maxwell, *J. Mol. Biol.* **2001**, *309*, 1219-1231.

SUPPORTING INFORMATION

Additional supporting information may be found online in the Supporting Information section.

How to cite this article: Abdel-Mohsen HT, Abood A, Flanagan KJ, Meindl A, Senge MO, El Diwani HI. Synthesis, crystal structure, and ADME prediction studies of novel imidazopyrimidines as antibacterial and cytotoxic agents. *Arch Pharm Chem Life Sci.* 2020;e1900271.
<https://doi.org/10.1002/ardp.201900271>